

Influence of giant reed (Arundo donax L.) culms processing procedure on physicochemical, rheological, and thermomechanical properties of polyethylene composite

Suarez , L., Hanna, P. R., Ortega, Z., Barczewski, M., Kosmela, P., Millar, B., & Cunningham, E. (2024). Influence of giant reed (Arundo donax L.) culms processing procedure on physicochemical, rheological, and thermomechanical properties of polyethylene composite. *Journal of Natural Fibers*, *21*(1), Article 2296909 . https://doi.org/10.1080/15440478.2023.2296909

Published in:
Journal of Natural Fibers

Document Version:
Publisher's PDF, also known as Version of record

Queen's University Belfast - Research Portal:
Link to publication record in Queen's University Belfast Research Portal

Publisher rights
Copyright 2024 the authors.
This is an open access article published under a Creative Commons Attribution License (https://creativecommons.org/licenses/by/4.0/), which permits unrestricted use, distribution and reproduction in any medium, provided the author and source are cited.

General rights
Copyright for the publications made accessible via the Queen's University Belfast Research Portal is retained by the author(s) and / or other copyright owners and it is a condition of accessing these publications that users recognise and abide by the legal requirements associated with these rights.

Take down policy
The Research Portal is Queen's institutional repository that provides access to Queen's research output. Every effort has been made to ensure that content in the Research Portal does not infringe any person's rights, or applicable UK laws. If you discover content in the Research Portal that you believe breaches copyright or violates any law, please contact openaccess@qub.ac.uk.

Open Access
This research has been made openly available by Queen's academics and its Open Research team. We would love to hear how access to this research benefits you. – Share your feedback with us: http://go.qub.ac.uk/oa-feedback

Download date:07. Oct. 2026

Taylor & Francis
Taylor & Francis Group

Journal of Natural Fibers

ISSN: (Print) (Online) Journal homepage: https://www.tandfonline.com/loi/wjnf20

Influence of Giant Reed (*Arundo Donax L.*) Culms Processing Procedure on Physicochemical, Rheological, and Thermomechanical Properties of Polyethylene Composites

Luis Suárez, Paul R. Hanna, Zaida Ortega, Mateusz Barczewski, Paulina Kosmela, Bronagh Millar & Eoin Cunningham

To cite this article: Luis Suárez, Paul R. Hanna, Zaida Ortega, Mateusz Barczewski, Paulina Kosmela, Bronagh Millar & Eoin Cunningham (2024) Influence of Giant Reed (*Arundo Donax L.*) Culms Processing Procedure on Physicochemical, Rheological, and Thermomechanical Properties of Polyethylene Composites, Journal of Natural Fibers, 21:1, 2296909, DOI: 10.1080/15440478.2023.2296909

To link to this article: https://doi.org/10.1080/15440478.2023.2296909

© 2024 The Author(s). Published with license by Taylor & Francis Group, LLC.

View supplementary material

Published online: 05 Jan 2024.

Submit your article to this journal

View related articles

View Crossmark data

Full Terms & Conditions of access and use can be found at
https://www.tandfonline.com/action/journalInformation?journalCode=wjnf20

JOURNAL OF NATURAL FIBERS
2024, VOL. 21, NO. 1, 2296909
https://doi.org/10.1080/15440478.2023.2296909

Taylor & Francis
Taylor & Francis Group

OPEN ACCESS Check for updates

Influence of Giant Reed (*Arundo Donax L.*) Culms Processing Procedure on Physicochemical, Rheological, and Thermomechanical Properties of Polyethylene Composites

Luis Suárez[a], Paul R. Hanna[b], Zaida Ortega[c], Mateusz Barczewski[d], Paulina Kosmela[e], Bronagh Millar[b], and Eoin Cunningham[f]

[a]Departamento de Ingeniería Mecánica, Universidad de Las Palmas de Gran Canaria, Las Palmas, Spain; [b]Polymer Processing Research Centre, Queen's University of Belfast, Belfast, UK; [c]Departamento de Ingeniería de Procesos, Universidad de Las Palmas de Gran Canaria, Las Palmas, Spain; [d]Institute of Materials Technology, Faculty of Mechanical Engineering, Poznan University of Technology, Poznań, Poland; [e]Department of Polymer Technology, Gdansk University of Technology, Gdańsk, Poland; [f]School of Mechanical and Aerospace Engineering, Queen's University Belfast, Belfast, UK

ABSTRACT

Giant reed (*Arundo donax* L.) is a plant species with a high growth rate and low requirements, which makes it particularly interesting for the production of different bioproducts, including natural fibers. This work assesses the use of fibers obtained from reed culms as reinforcement for a high-density polyethylene (HDPE) matrix. Two different lignocellulosic materials were used: i) shredded culms and ii) fibers obtained by culms processing, which have not been reported yet in literature as fillers for thermoplastic materials. A good stress transfer for the fibrous composites was observed, with significant increases in mechanical properties; composites with 20% fiber provided a tensile elastic modulus of almost 1900 MPa (78% increase versus neat HDPE) and a flexural one of 1500 MPa (100% increase), with an improvement of 15% in impact strength. On the other hand, composites with 20% shredded biomass increased by 50% the tensile elastic modulus (reaching 1560 MPa) and the flexural one (up to 1500 MPa), without significant changes in impact strength. The type of filler is more than its ratio; composites containing fibers resulted in a higher performance than the ones with shredded materials due to the higher aspect ratio of fibers.

KEYWORDS

Arundo donax; giant reed; biomass; fibers; composites; HDPE; characterization; injection molding

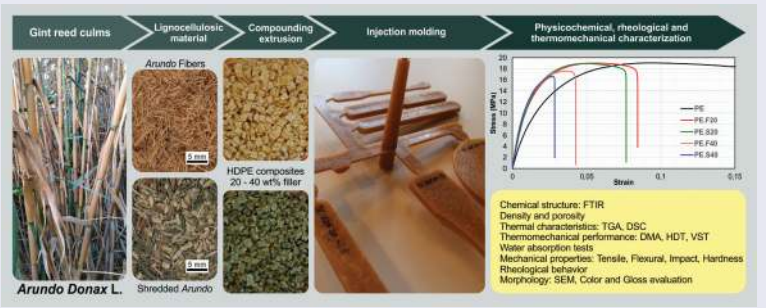
关键词

Arundo donax; 巨大的芦苇; 生物量; 纤维; 复合材料; HDPE; 刻画; 注射成型

CONTACT Zaida Ortega zaida.ortega@ulpgc.es Departamento de Ingeniería de Procesos, Universidad de Las Palmas de Gran Canaria, Las Palmas, Spain

Supplemental data for this article can be accessed online at https://doi.org/10.1080/15440478.2023.2296909

© 2024 The Author(s). Published with license by Taylor & Francis Group, LLC.
This is an Open Access article distributed under the terms of the Creative Commons Attribution License (http://creativecommons.org/licenses/by/4.0/), which permits unrestricted use, distribution, and reproduction in any medium, provided the original work is properly cited. The terms on which this article has been published allow the posting of the Accepted Manuscript in a repository by the author(s) or with their consent.



摘要

巨型芦苇（Arundo donax L.）是一种生长速率高、要求低的植物，这使得它对生产包括天然纤维在内的不同生物产品特别感兴趣. 这项工作评估了从芦苇秆中获得的纤维作为高密度聚乙烯（HDPE）基体的增强材料的用途. 使用了两种不同的木质纤维素材料: i）切碎的秆和ii）通过秆加工获得的纤维，这些纤维在文献中尚未被报道为热塑性材料的填料. 观察到纤维复合材料具有良好的应力传递，机械性能显著提高; 含20%纤维的复合材料的拉伸弹性模量几乎为1900MPa（与纯HDPE相比增加了78%），弯曲弹性模量为1500MPa（增加了100%），冲击强度提高了15%. 另一方面，具有20%切碎生物质的复合材料的拉伸弹性模量（达到1560MPa）和弯曲弹性模量（高达1500MPa）增加了50%，而冲击强度没有显著变化. 填料的种类多于其配比; 含有纤维的复合材料由于纤维的高纵横比而比含有切碎材料的复合材料具有更高的性能.

Introduction

Arundo donax L. is a perennial Grass from the *Gramineae* family, probably with East Asia origin (Jensen et al. 2018). This plant shows a high growth rate and produces an impressive amount of biomass, which currently has very limited use. Several works have demonstrated the potential of this plant for the biorefinery industry (Copani et al. 2013; Cosentino et al. 2014, 2016; Jensen et al. 2018; Licursi et al. 2015, 2018; Ortega et al. 2023) and it is considered as an energy crop because of its potential to produce bioethanol, bioenergy, or green products following a biorefineries scheme. The use of a cascade biorefinery process is an exciting strategy to maximize the environmental and economic benefits of lignocellulosic materials used within industrial applications; in this approach, the different fractions of the material could be separated for their further use. One interesting product that can be obtained from such industries are cellulose fibers for composites obtaining, while also exploiting the remaining fractions for the obtaining of other products, such as sugars for a later fermentation, antioxidants or bio-char (Ortega et al. 2023).

Some authors have proposed using giant reed as a raw material to obtain natural fibers, although not many publications study the manufacturing of composites using fibers. Most literature related to composites production from *Arundo* focuses on particleboard production (Andreu-Rodriguez et al. 2013; Barreca et al. 2019; Ferrández Villena et al. 2020; Ferrandez-Garcia et al. 2019; Ferrandez-García et al. 2020; Ferrández-García et al. 2012; García-Ortuño et al. 2011). In such works, the lignocellulosic material is ground and blended in up to 40% by weight with a thermoset resin or natural binders, such as citric acid (Baquero Basto, Monsalve Alarcón, and Sánchez Cruz 2018; Dahmardeh Ghalehno et al. 2010; Ferrandez-Garcia et al. 2019; Ferrandez-García et al. 2020); the medium-density boards obtained show properties within the range of other materials used as insulating material in the construction or furniture sector.

As explained in a previous review paper from authors (Suárez et al. 2023,) three methods are mainly used for reed processing: grinding (Bessa et al. 2020, 2021; Fiore et al. 2014, 2014) rudimentary

scraping to obtain bast fibers (Fiore et al. 2014; Ortega et al. 2021; Scalici, Fiore, and Valenza 2016; Suárez et al. 2021, 2022) or the combination of a chemical soaking and mechanical scraping to get thinner and stiffer fibers (Suárez et al. 2023). Purely chemical methods have also been explored in the literature for the separation of microcrystalline cellulose (Shatalov and Pereira 2013)(p) (Barana et al. 2016; Tarchoun et al. 2019). From the studies reported in the literature, it can be concluded that the initial preparation of the filler derived from this plant and the applied mechanical and chemical modification procedure significantly affect the properties of composites produced. For example, acid hydrolysis allows for the removal of hemicellulose and the obtaining of a pulp with high cellulose content (Shatalov and Pereira 2013; Tarchoun et al. 2019) while the use of alkali results in the removal of lignin and the obtaining of a material with about 50% cellulose (Barana et al. 2016; Martínez-Sanz et al. 2018). The procedure applied for obtaining the fibers in this research work combines a chemical and a mechanical approach (Suárez et al. 2023) for the obtaining of fibers with high aspect ratio and high cellulose content, close to 70%.

Epoxy-based composites have been studied at different fiber loadings; for example, the addition of 10% in weight of bast fibers showed improved tensile modulus of the epoxy matrix, while tensile and flexural strength were reduced due to a low compatibility between the lignocellulosic material and the resin. To overcome this, plasma treatment has been applied to the fibers (Scalici, Fiore, and Valenza 2016) and it has been found that 5% loading increased the flexural modulus by up to 80% and flexural strength by almost 40%. The lack of compatibility between both materials not only prevents the transmission of the applied force between both materials but also results in voids formation, which reduce the effective area of the test part. Apart from plasma, an alkaline treatment based on NaOH or the silanization (Bessa et al. 2020) of fibers has been proposed for their use in unsaturated polyester or bisphenol-based matrices. For polyester, composites at 40% loading (in volume) were prepared, resulting in an improvement of tensile and flexural properties (Chikouche et al. 2015).

Some studies have also been performed using thermoplastic materials as a matrix. For example, PLA-composites with up to 20% of *Arundo* ground culms were prepared by injection molding, with tensile and flexural elastic moduli rising with the increased content of lignocellulosic material, while the strength was reduced in both tests. Further studies using *Arundo* to produce polymer composites by injection molding have not been found in the literature, therefore demonstrating the novelty of this work. The present paper shows the results obtained for composites with 20% and 40% *Arundo* fibers, which have only been obtained with this plant by compression molding (Suárez et al. 2021). In this work, polyethylene (PE) and polypropylene (PP) were used as matrices, resulting in an increase in elastic modulus and a decrease in tensile and flexural strength. Rotationally-molded composites with *Arundo* resulted in similar behavior, although a lower rate of filler was used due to the process sensitivity to the introduction of non-polymeric materials (Suárez et al. 2022). In addition, the literature reviewed typically used ground material or bast fibers obtained from rudimentary procedures, with lower cellulose content and mechanical properties than the fibers used in this research.

In this paper, the properties of composites obtained with shredded culms and fibers obtained by combined chemical and mechanical methods are assessed. Giant reed fibers used in this research show a high cellulose content (around 68%, in the range of flax or hemp (Henrique et al. 2015) with a crystallinity index over 65%, and thermal degradation temperature above 230°C, similar to other commonly used fibers in the composites sector, such as jute, abaca, or hemp (Fiore, Scalici, and Valenza 2014; Kabir et al. 2012; Ortega et al. 2013). The shredded material also shows good thermal stability for its processing into a HDPE matrix (Suárez et al. 2023). From the energy point of view, it is beneficial to produce composites based on the less processed plant raw materials. Therefore, this research work aims at contributing to the achievement of the EU-green deal strategy objectives and the sustainable development goals, by the obtaining of composites with good performance and an expected improved environmental character due to the partial substitution of a polymer matrix with a renewable material of lignocellulose origin. Other authors have reported some few results on the use of giant reed materials in thermoplastic processes, although with a different starting material. To the best of authors knowledge, no references in literature have used the two lignocellulose materials

reported in this work: fibers obtained from a chemo-mechanical procedure of giant reed culms, with high cellulose content, and shredded material from the entire aerial parts of the reed, with lower cellulose and higher hemicellulose contents. A comprehensive correlation assessment between the method of obtaining the giant reed-based fillers and the processing, physicochemical, thermal, and thermomechanical properties of injection-molded thermoplastic composites manufactured with their use was presented.

Materials and methods

Materials

High-density polyethylene (HDPE), grade HD6081 from Total was used. This polymer exhibits a melt flow index (MFI) of 8 g/10 min (190°C/2.16 kg) and a density of 960 kg/m^3, according to the manufacturer's datasheet.

Fibers and shredded material from *Arundo* culms were prepared as explained in previous work (Suárez et al. 2023). In short, shredded material was prepared by grinding the aerial parts of the plant (culms and leaves) and washing them with water. Fibers were obtained after soaking culms in a 1N NaOH solution for around 1 week (3 l of solution per kg of biomass), with further processing by a series of rolling mills to separate the fibers from the softer material. Finally, fibers were cut to approximately 3 mm in length.

The composites are named after the type of lignocellulosic material used and its content (in weight %); for example, PE.F20 stands for composites with 20% of fibers, while PE.S20 refers to composites with 20% of shredded material. Table 1 lists the samples' full names and information about their composition.

Composites preparation

The materials used were dried overnight before compounding: lignocellulosic fibers at 105°C and HDPE at 60°C. Composites were prepared in a ThermoScientific Process11 twin screw-extruder (configuration shown in Figure 1), with the following temperature profile: 170-175-175-185-185-175-165-165°C (from hopper to die). The screw speed at 100 rpm.

Before injection molding, the materials were dried at 60°C overnight with dry air (dewpoint of −40°C). ISO mechanical test specimens were manufactured using an Arburg 320S injection molding machine. The following temperature profile, from back to nozzle, was used: 175-180-185-185-190°C, while mold temperature was 30°C, and cooling time was 15 s. The back pressure was 5 MPa, the holding pressure was 50 MPa and the dosage volume of 50 cm^3. Switchover pressure was recorded for every molding and averaged for the various composites.

Characterization

Different characterization tests were performed on the pellets and the injection-molded parts. For the pellets, chemical structure, melt flow index, and thermal analysis (thermogravimetry and differential scanning calorimetry) were assessed. For molded parts, density, water absorption, mechanical testing,

Table 1. Materials prepared and their markings.

Short name	Formulation
PE	HDPE
PE.S20	HDPE +20% shredded *Arundo*
PE.S40	HDPE +40% shredded *Arundo*
PE.F20	HDPE +20% *Arundo* fiber
PE.F40	HDPE +40% *Arundo* fiber

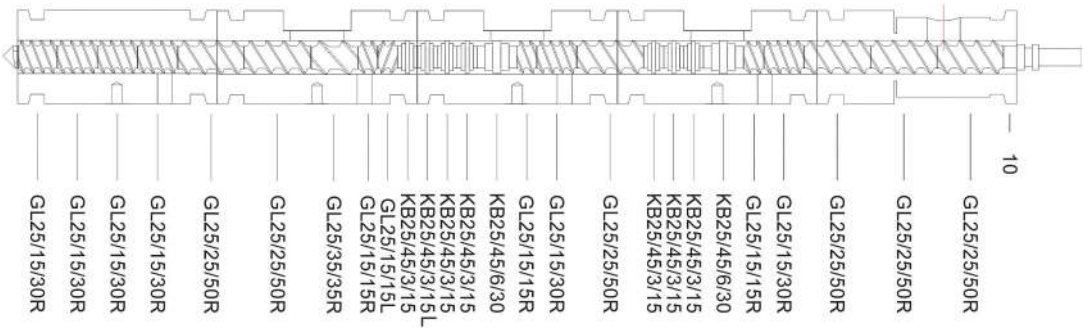


Figure 1. Extruder screw configuration with three different mixing and kneading zones.

dynamic mechanical analysis, rheological behavior, heat deflection and Vicat softening temperatures (HDT and VST), and microscopic structure were analyzed.

Fourier Transform Infrared (FTIR) spectra were obtained in a Spectrum 100 spectrophotometer from Perkin Elmer, under Attenuated Total Reflectance (ATR) mode with a zinc selenide single bounce crystal, recording 64 scans per spectra at a resolution of 4 cm^{-1}, in the wavelengths between 4000 and 600 cm^{-1}.

The Melt Flow Index (MFI) of composite materials was obtained following ISO 1133, in a 7053 apparatus from Kayeness Inc (Dynisco Company), using a load of 2.16 kg and a temperature of 190°C.

Thermogravimetric analysis (TGA) was performed in a Netzsch TG 209F1 Libra device, using alumina crucibles and samples nominally of 10 ± 0.2 mg, under nitrogen atmosphere. The tests were conducted at a heating rate of 10°C/min, from 30°C to 900°C.

Heat deflection temperature (HDT) was obtained for injection-molded samples according to ISO 75 standard (heating rate of 120°C/h and 1.8 MPa load). Vicat softening temperature (VST) was measured following ISO 306 B50 standard, at a heating rate of 50°C/h and a loading of 50 N. For both tests TPC/3 TOP VST/HDT apparatus was used. For each series, at least three measurements were made to average the results.

The thermal behavior of materials was determined by differential scanning calorimetry (DSC). The analyses were conducted in a Perkin Elmer DSC 6 device under nitrogen atmosphere and aluminum sealed crucibles. Samples nominally of 10 ± 0.2 mg were prepared for these tests. The measurements were performed from 30°C to 200°C at 10°C/min, with two heating cycles. The temperatures for melting at both heating cycles (Tm_1 and Tm_2, respectively) and crystallization (T_c) from the cooling step were determined. Three replicas were performed for each material sample, and results are expressed as average values, also providing standard deviations. Finally, the melting and crystallization enthalpies (ΔHm_1, ΔHm_2, and ΔHc) were also calculated and employed to obtain the degree of crystallinity (χ):

$$\chi = \frac{1}{1 - m_f} \cdot \frac{\Delta H_m}{\Delta H_0} \cdot 100 \tag{1}$$

where ΔH_0 is the enthalpy for a HDPE crystalline sample (293 J/g) (Balasuriya, Ye, and Mai 2003,) and m_f is the mass rate of the lignocellulose (20% and 40% for composites).

The density of the prepared materials was measured following the Archimedes principle, as specified in ISO 1183 standard, using methanol medium at room temperature, in a LA620P precision balance from Sartorius AG Germany. Five measurements were performed per sample, giving the results as average value and standard deviation. The theoretical density of each formulation was calculated following the rule of mixtures (equation 2):

$$\rho_C = \rho_f \cdot V_f + \rho_m \cdot (1 - V_f) \tag{2}$$

Where V_f is the mass ratio of the lignocellulosic material, and ρ_c, ρ_f, and ρ_m, the density of the composite (theoretical), fiber and matrix. These values were further used to calculate the composite porosity (P) (equation 3), by comparing the theoretical and experimental values obtained:

$$P(\%) = \frac{\rho_{theo} - \rho_{exp}}{\rho_{theo}} \cdot 100 \tag{3}$$

Water absorption was carried out according to ISO 62:2008, immersing the specimens in deionized water and weighing them periodically until achieving a constant mass. The water absorption (W) was calculated using the following equation:

$$W(\%) = \frac{W_t - W_0}{W_0} \cdot 100 \tag{4}$$

where W_0 is the initial mass of the sample, W_t the mass of the sample at t time. Three replicates per sample were assessed.

The kinetics of water uptake can be obtained using Fick's law:

$$D = \pi \cdot \left(\frac{k \cdot h}{4 \cdot W_m}\right)^2 \tag{5}$$

Where D is the diffusion coefficient (m (Copani et al. 2013)/s), h is the thickness of the original sample, W_m is the maximum moisture absorbed by the sample and k is the initial slope of the curve of water uptake versus $t^{1/2}$, as described by equation 6 (Bazan et al. 2020):

$$k = \frac{W_2 - W_1}{\sqrt{t_2} - \sqrt{t_1}} \tag{6}$$

If the moisture uptake for each measurement taken is compared with the maximum water uptake of each sample, the parameters n, associated with the diffusion mode, and k, related to the interaction between the material and the water, can be calculated as (George, Bhagawan, and Thomas 1998):

$$\frac{W_t}{W_m} = k \cdot t^n \tag{7}$$

The mechanical properties of composites (tensile, flexural, impact, and hardness) were determined as follows: i) tensile properties: ISO 527–2:2012, at a rate of 10 mm/min for ultimate tensile strength and 2 mm/min for elastic modulus, ii) flexural properties: ISO 178:2019, with 64 mm between cantilevers, determining the elastic modulus and flexural strength, at the same rates defined for tensile tests. These tests were made in a LS5 universal testing machine (Lloyd), with a cell load of 500 N for modulus and of 5 kN for strength, with 5 replicates per test. iii) Charpy impact tests: UNE-EN ISO 179–1/1eA:2019, with a 7.5 J pendulum and an impact rate of 3.7 m/s in a Ceast Resil impactor P/N 6958.000, using notched samples. Ten replicates were used for this assay. iv) Hardness: ISO 2039 standard, conducting the tests in a KB Prüftechnik device (ball indentation hardness test), with a minimum of 7 measurements per each material series. Results for all properties are given as average values and standard deviation (SD).

Thermomechanical properties of the different materials were evaluated by Dynamic Mechanical Thermal Analysis (DMTA) in a Tritec 2000 device, from Triton Technology, under single cantilever bending method. A strain of 10 μm was applied at 1 Hz frequency, in the temperature range between −100°C and 100°C, at a heating of 2°C/min.

Rheological behavior was assessed using an AR G2 oscillatory rheometer from TA instruments, using 25 mm diameter parallel plates. The experiments were performed at 190°C, with 2.5 mm gap and in a nitrogen atmosphere. Preliminary tests were performed using the strain sweep mode, in order to ensure later experiments are performed in the linear viscoelastic (LVE) region. In these tests, strain

was varied between 0.1% and 5%. Angular frequency sweeps were performed at 0.5% strain, in the LVE region, in the range of 0.01 to 100 rad/s.

The analysis of rheological evaluation was supplemented with experiments conducted using a capillary rheometer Dynisco LCR 7000, at 190°C, as for oscillatory measurements. This test, performed with a capillary die with a diameter of D = 2 mm and L/D = 20, allowed determining the effect of the lignocellulosic materials on the rheological properties of the HDPE matrix. The high value of L/D made the Bagley correction to be. T changes in the rheological behavior were analyzed by means of the apparent shear stress; the dependence between the apparent melt viscosity (η) and the apparent shear rate ($\dot{\gamma}$) (in double logarithmic scale) allow to describe the viscosity curves in the non-Newtonian range a the power-law (Gai and Cao 2013) (equation 8):

$$\eta = K(\dot{\gamma})^{n-1} \tag{8}$$

Where K is the consistency coefficient, and n is the power law index (Djellali et al. 2015).

Scanning electron microscopy (SEM) observations were performed over the samples surface and fractured sections of tensile specimens, with the aim of determining the distribution of the filler in the matrix and describe an interaction between filler and matrix. SEM observations were performed in a Hitachi FlexSEM 1000, at different magnifications and an accelerating voltage of 5 kV, over previously gold-sputtered samples.

The color of the samples was assessed by optical spectroscopy, using a HunterLab Miniscan MS/S-4000S spectrophotometer, following the procedure specified by the International Commission on Illumination (CIE) L*a*b* coordinates. According to this system, L* is related to the color lightness (black: L* = 0, white: L* = 100), a* refers to green(−) and red(+), and, finally, b* measures blue(−) and yellow(+) The measurements were done by placing the samples in a specially designed light trap chamber. The total color difference parameter (ΔE*) is defined as (Chorobiński, Skowroński, and Bieliński 2019):

$$\Delta E^* = \left[(\Delta L^*)^2 + (\Delta a^*)^2 + (\Delta b^*)^2\right]^{0.5} \tag{9}$$

Finally, the measurement of the gloss of the surface of samples was performed using the TestAn DT 268 glossmeter, according to ISO 2813: 2001 at an angle of 20, 60, and 85° of the apertures of the image of the light source and the receiver. The presented results are mean values taken from 20 measurements.

Results

Chemical structure – FTIR

Figure 2a, b shows the FTIR spectra for the different materials used in this work: i) *Arundo* fibers and shredded *Arundo* plants (Figure 2a), II) PE, iii) 20% composites, and iv) 40% composites (Figure 2b). As already analyzed in previous work (Suárez et al. 2023,) the shredded material shows peaks associated to hemicellulose and lignin, which disappear or are reduced for fiber samples, due to the extraction procedure which was followed. Composites for both types of materials show almost overlapped spectra, closer to PE for the lower loadings. Composites with 40% of lignocellulosic material start showing some of the characteristic bands of such materials, namely around 3600–3000 cm^{-1}, related to O-H stretching, and 1200–850 cm^{-1}, characteristic of C=O bonds in cellulosic compounds.

The double peak at 2916 and 2848 cm^{-1} are related to C-H bonds (symmetric and asymmetric vibrations) from the polyethylene chain, although is also present in the lignocellulosic materials (with less intensity) and attributed to hemicellulose so more intense for shredded material than for the fiber. The peaks at 1472 and 729 cm^{-1} are related to C-H stretching in HDPE, and so are also found for the composites. It can be observed that the introduction of the lignocellulosic materials modifies the signal of neat HDPE, with the appearance of bands due to the giant reed materials. Other authors have

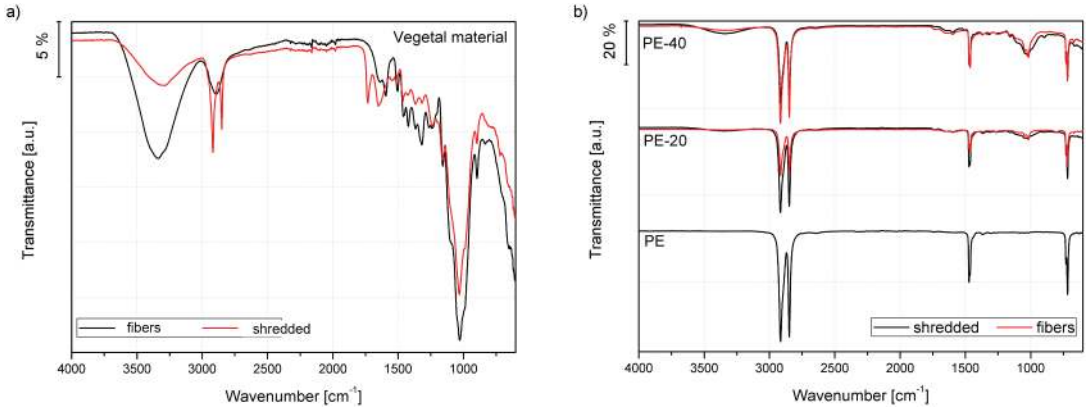


Figure 2. FTIR spectra of the fillers (a) and injection molded samples (b).

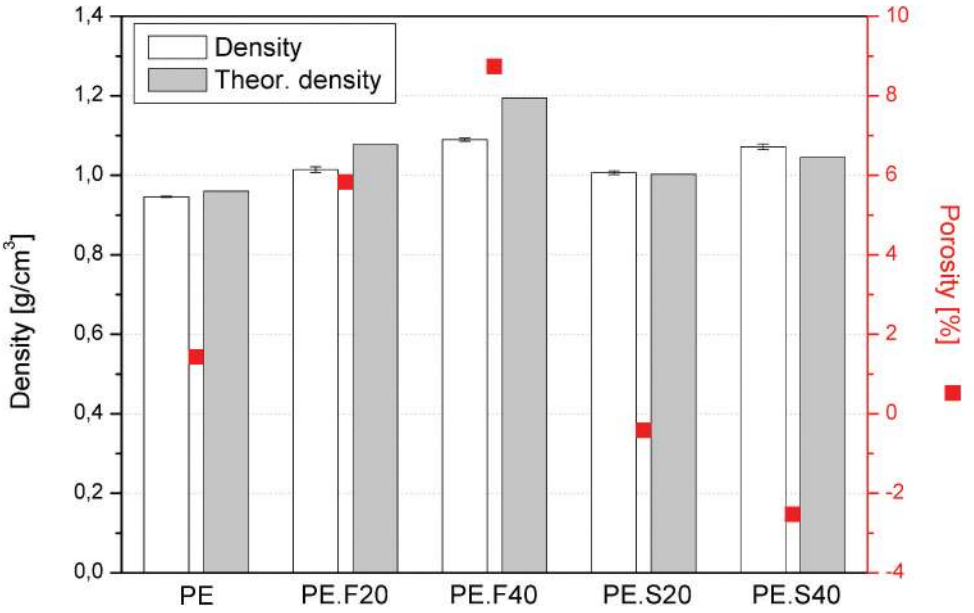


Figure 3. The porosity of PE-*arundo* composites based on measured and theoretical density.

reported similar modifications, especially for high filler loadings (Hejna et al. 2020; Mendes et al. 2021).

Density and porosity assessment

Figure 3 shows the values for theoretical and experimental densities of the composites and the porosity calculated by comparing them. Density values increase with the increasing content of lignocellulosic material in the composite. If comparing the density values obtained in the methanol assay and the theoretical ones (Equation 2), the porosity values could be obtained (Equation 3). It can be seen that the values for theoretical and experimental density for composites with shredded materials are pretty similar, so the porosity values can be considered zero. The values obtained were −0.5 and −2.5% for 20% and 40% composites, possibly due to some overpacking during injection molding or the standard deviation of the measurements taken. Porosity values for composites with fibers are 5.8 and 8.7%, for

20% and 40% fiber content, respectively, which can still be considered acceptable, especially for such high lignocellulosic contents.

Thermal behavior

Thermogravimetry

Figure 4 shows the thermogravimetric (TG) and derivative (DTG) curves obtained for the polyethylene and its composites. The thermal stability for 20% and 40% composites is similar, regardless of the type of lignocellulose material used. The residual mass at the end of the assay is also found in similar proportions for both sets of composites and are due to the inorganic compounds in the biomass, i.e., about 20% (Suárez et al. 2023). From DTG, the most significant peak is related to the PE decomposition, taking place at about 460°C, while for composites, there is also a smaller one, between 220°C and 360°C, due to the cellulose degradation. For composite materials with shredded *Arundo*, as also observed for the material itself, a small shoulder at about 290°C is found due to hemicellulose pyrolysis. A similar behavior is described in the literature for composites with lignocellulose-derived fillers. All composites are thermally stable until reaching about 240°C, 50°C above the processing temperature, which indicates a temperature-wide processability window for such materials (Mazzanti, Mollica, and El Kissi 2016). For instance, 5% weight loss happens at about 420°C for neat PE, about 290°C for 20% composites, and 270°C for 40% ones. Similar results are found in literature, with degradation starting at 214°C for hemp fibers at 40% in a polypropylene matrix or 262°C for 30 wt.% wood fibers-filled HDPE composites (Monteiro et al. 2012). There is a direct correlation between the amount of lignocellulosic material introduced and the weight loss, as also observed in Figure 4a. Some authors have proposed using TG and DTG curves to calculate the proportion of filler in the composite experimentally; following the procedure set by Nabinejad et al (Nabinejad et al. 2023) less than 10% difference between the theoretical and the experimental ratios are found: 21.7% and 20.9% for 20% composites (fiber and shredded, respectively), and 42.8% and 39.1% for 40%.

Differential scanning calorimetry

For polyethylene samples, the melting temperature is around 133°C, finding a slight increase for 20% composites. Melting and crystallization peaks are not altered because of the lignocellulose materials introduction, and no differences between the first and second heating cycles could be observed, neither in temperatures of the phase transitions nor in crystallinity values (Table 2). Other authors have reported similar behavior for HDPE-based composites: negligible difference in melting temperatures, although with reductions in enthalpies (Andrzejewski et al. 2020; Dolçà et al. 2022).

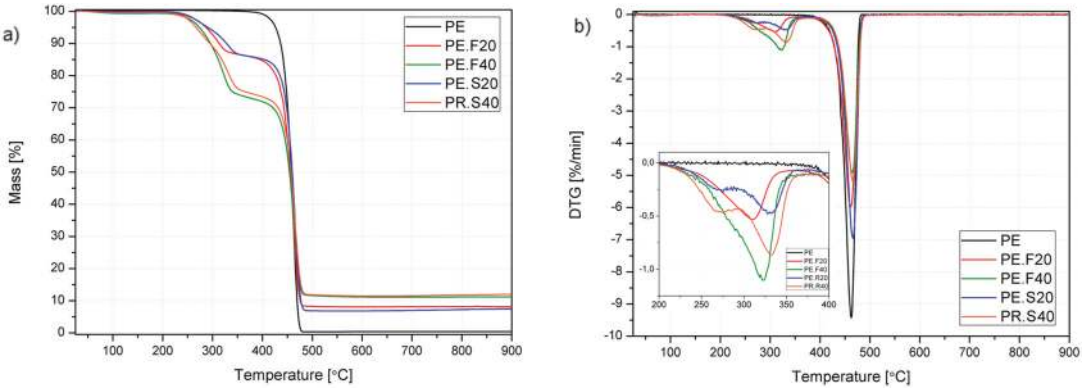


Figure 4. a) TG curve for the different materials and b) DTG curve.

Table 2. Thermal parameters for HDPE and its composites from DSC tests.

Material	Tm_1 [°C]	Tm_2 [°C]	T_C [°C]	ΔH_{m1} [J/g]	ΔH_{m2} [J/g]	ΔH_C [J/g]	χ_1 [%]	χ_2 [%]
HDPE	132.7 ± 0.3	135.3 ± 0.9	112.9 ± 0.0	175.4 ± 13.5	172.6 ± 8.2	193.3 ± 21.2	59.9 ± 4.6	58.9 ± 2.8
PE.F20	136.9 ± 0.4	134.7 ± 1.0	111.5 ± 0.0	118.7 ± 12.9	125.8 ± 11.2	135.8 ± 9.3	50.6 ± 5.5	53.7 ± 4.8
PE.F40	132.7 ± 0.4	133.9 ± 0.7	113.1 ± 0.7	108.6 ± 22.8	109.5 ± 18,4	108.4 ± 12.12	61.8 ± 13.0	62.3 ± 10.5
PE.S20	137.2 ± 0.6	136.2 ± 1.4	111.1 ± 0.7	119.4 ± 0.4	128.4 ± 3.1	140.8 ± 4.0	50.9 ± 0.2	54.8 ± 1.3
PE.S40	133.0 ± 0.9	135.0 ± 1.9	112.1 ± 1.4	76.4 ± 17.1	79.8 ± 15.7	82.5 ± 15.3	43.5 ± 9.7	45.5 ± 8.9

The crystallinity seems to decrease with the incorporation of the lignocellulosic material, except for 40% fiber composites, which shows a value close to that of neat PE (although it also gives a higher deviation). The high content of such fibers could counteract the reduction of crystallinity due to the incorporation of the lignocellulosic material, with relatively high crystallinity (close to 70% (Suárez et al. 2023). Besides, cellulose can act as an active nucleation center (Dolçà et al. 2022) and fibers contain over 65% of cellulose, according to previous research conducted. The geometry of the fillers can also influence their effect on crystallization; usually, smaller particles lead to higher crystallinity (Dolza et al. 2021).

On the contrary, incorporating lignocellulosic materials into the HDPE matrix can hinder the crystallization process, especially at lower loadings, due to the restrained mobility of the polymer chains (Fendler et al. 2007). An increase in melting temperature for 20% composites has been observed for bamboo-HDPE composites at the same loadings, with a reduction in melting enthalpy also and, thus, in crystallinity (Mohanty and Nayak 2010; Wang et al. 2014). There is no clear trend in the literature about the effect of lignocellulosic fillers in HDPE: some authors found reductions in crystallinity (Fendler et al. 2007,) while others have found increases (Jaramillo et al. 2021). No significant changes have been also reported (Mendes et al. 2021,) usually getting crystallinity values typically close to 50% for composites with natural fillers (Andrzejewski et al. 2020) (see supplementary figure S1).

Thermomechanical behavior

The introduction of lignocellulosic materials can effectively increase the range of application of the neat HDPE, as both parameters measured, heat deflection temperature (HDT) and Vicat softening temperature (VST), increased (Table 3). It was found that higher ratios of biomass led to higher thermomechanical stability of composites. The filler type showed a lower influence on the HDT or the VST than the percentage of filler used. Despite slight differences higher statically assessed thermomechanical stability values were noted for *Arundo* fibers composites compared to *Arundo* shredded filler. This effect was noticeable in the samples subjected to point loading and three-point bending. The values of HDT and VST correlate with the changes of mechanical properties (hardness and flexural elasticity modulus described later in Section 3.5), and described in the literature for polyethylene-based composites (Schellenberg 1997). It results from better dispersion of fibers in the polymer matrix and higher reinforcing efficiency associated with the increased shape factor of fibrous filler (aspect ratio about 4 for fibers, with fiber lengths about 0.8 mm; particle size for shredded filler is around 0.45 mm). Based on the DSC analysis, the increase in resistance to static load in the high-temperature range should not be associated to the change in the crystallinity. The HDPE composites

Table 3. Heat deflection (HDT) and Vicat softening temperatures (VST).

Material	HDT [°C]	VST [°C]
HDPE	41.00 ± 1.03	72.32 ± 1.34
PE.F20	57.27 ± 1.03	81.30 ± 0.80
PE.F40	72.88 ± 1.31	85.75 ± 1.64
PE.S20	55.31 ± 1.60	78.93 ± 0.22
PE.S40	67.51 ± 3.80	83.40 ± 0.93

produced exhibit a HDT close to PP or PET, with increases of about 50% regarding the neat HDPE. The dynamic mechanical analysis also observes this improved thermal resistance (section 3.6).

Water absorption tests

Figure 5a clearly shows that higher lignocellulosic loadings result in higher water absorption. In contrast, HDPE water absorption is almost negligible. Each point is the average value of three measurements. Moisture uptake equilibrates at a maximum of 2% for 20% composites but is increased by over 400% for 40% loadings, reaching up to 9% after the 28 days of the assay. As the materials used in this work are hydrophilic, an increase in water uptake for the composites was expected. The parts' thickness was measured at the beginning and the end of the assay to determine their swelling. This parameter follows a similar trend to water uptake, i.e., higher loadings increased swelling. Composites with fibers show higher swelling values than composites with shredded *Arundo*, following the same trend as water uptake. This increased water uptake by fibers is surprising, as a lesser hydrophilic character was expected due to the higher cellulose and lower hemicellulose contents of fibers compared to shredded material [22]. However, the morphology of the materials also plays an important role; fibers are thinner and have a higher aspect ratio than shredded material, and so have a higher area exposed, which might explain this behavior. This observation correlates with the porosity values obtained by comparing theoretical and experimental densities, the composites with higher porosity exhibited higher water uptake due to a larger number of entry points where water molecules could ingress, as well as having a higher internal free volume in which the hydrophilic cellulosic content could swell. The aspect of the formation of the polymeric skin layer on injection molded samples, depending on the nature of the flow of filled molten composite during forming, cannot also be omitted (Najafi, Tajvidi, and Chaharmahli 2006; Salasinska et al. 2016).

Mechanical properties could be modified by the hydration of the fibers and their swelling, which could partially debond the fiber from the matrix, thus reducing the stress transfer between both phases. However, Bazan et al (Bazan et al. 2020). performed these studies with coconut and flax fibers, and despite the increase in water uptake and the swelling observed, no change in the mechanical properties of the composite was found, probably because of the high stability of the HDPE matrix.

From the data obtained, Fick's diffusion coefficient can be calculated using Equations (5-7). Figure 5b shows the representation of W_t/W_m versus time on a logarithmic scale, from which the parameter n is calculated. It can be seen that the data are linear in nature, except for neat PE, where the absorption values are so low that some data points were removed to get approximate values for such parameters (Table 4). The parameter n indicates the type of diffusion behavior that is taking place;

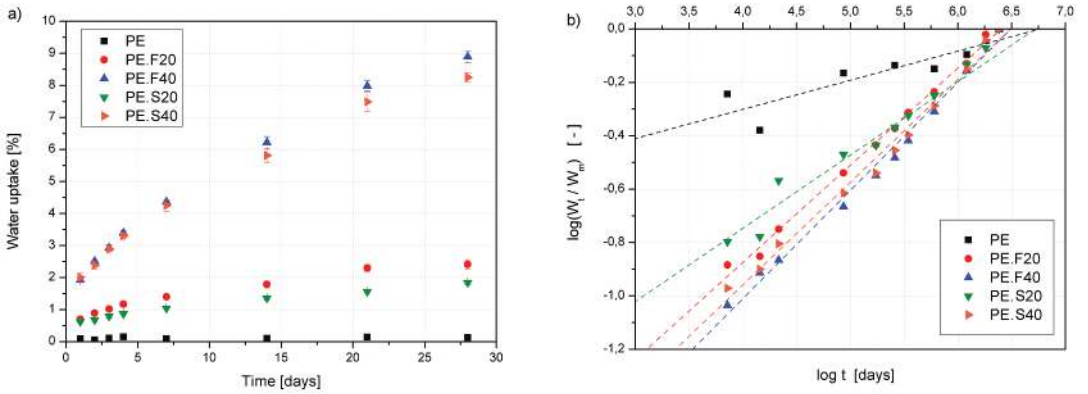


Figure 5. Results of moisture absorption. a) water uptake vs. time, b) calculation of Fick's law parameters (log W_t/W_m versus log time).

Table 4. Water uptake parameters of PE and its composites.

Material	D (m^2/s)	k (%/$s^{0.5}$)	n	Swelling (%)	Sorption (g/g)	Permeability (m^2/s)
PE	$3.62{\cdot}10^{-15}$	$3.53{\cdot}10^{-5}$	0.11	1.1	0.001	4.523·10 – 18
PE.F20	$3.22{\cdot}10^{-13}$	$1.61{\cdot}10^{-3}$	0.36	3.3	0.024	7.758·10 – 15
PE.F40	$2.32{\cdot}10^{-13}$	$4.98{\cdot}10^{-3}$	0.41	8.3	0.089	2.064·10 – 14
PE.S20	$3.56{\cdot}10^{-13}$	$1.10{\cdot}10^{-3}$	0.30	2.3	0.018	6.548·10 – 15
PE.S40	$3.46{\cdot}10^{-13}$	$4.88{\cdot}10^{-3}$	0.39	6.6	0.083	2.855·10 – 14

a value equal to 0.5 means a Fickian diffusion, while a value of 0.5–1.0 indicates an anomalous diffusion. In this case, it is observed that diffusion approaches the behavior predicted by Fick's law, with values ranging from 0.30 to 0.41, except for the neat HDPE. Other authors have found a similar behavior for pineapple leaf fibers (George, Bhagawan, and Thomas 1998) or wood flour (Bazan et al. 2020). Diffusion coefficients found for *Arundo* composites are higher than for neat PE and are of the same order for all composites. They are also in a similar range to other values found in the literature: $4{\cdot}10^{-13}$ m (Copani et al. 2013)/s for composites containing 40% rice hulls (Wang, Sain, and Cooper 2006,) or $3.6{\cdot}10^{-14}$ m (Copani et al. 2013)/s for composites with 30% pineapple fiber (George, Bhagawan, and Thomas 1998,) both in a PE matrix. Lower lignocellulose loadings lead to lower diffusion coefficients; for example, diffusion coefficients around $3{\cdot}10^{-12}$ m (Copani et al. 2013)/s are obtained for 12% wood, flax, or coconut fibers in HDPE-based composites, increased up to $6{\cdot}10^{-12}$ m (Copani et al. 2013)/s for the same percentage of basalt fibers (Bazan et al. 2020).

Some authors point out that moisture absorption in natural fiber composites is affected both by diffusion and percolation and so propose other parameters for the study of water uptake. George et al (George, Bhagawan, and Thomas 1998). calculated the sorption of water as the relationship between the mass of water absorbed by the sample and the weight of the sample itself and then introduced the permeability, obtained by the combination of sorption and diffusion (P=DxS).

Sorption and permeability coefficients increased with the content of lignocellulose in the composite, as also observed in the literature (George, Bhagawan, and Thomas 1998,) with values in the same range as those obtained by George et al. for pineapple fibers. Permeability for HDPE is about 1000 times lower than for composites due to the excellent barrier properties and hydrophobic character of this polymer.

Mechanical properties: tensile, flexural, impact, and hardness tests

As summarized in Table 5, 20% composites had the same tensile strength as neat HDPE, while 40% loadings led to a decrease of 8% and 14% for fiber and shredded material, respectively. This decrease could be related to the increased porosity of the composite, in the case of fiber material, and the reduced stress transfer between the matrix and the *Arundo*-derived materials. This may be due to a reduced compatibility between the fibers and the matrix or the formation of agglomerates. Therefore, for 20% composites, where tensile strength is not reduced, this suggests a sign of good adhesion between fiber and matrix and evidence of a good stress transfer between them (Fendler et al. 2007; Qiu, Endo, and Hirotsu 2004).

On the contrary, flexural strength increased for all composite samples, with no significant difference for the composites containing 20% of either fibers or shredded materials, where an increase in strength of about 15% was observed compared to neat HDPE. The most significant improvements are found for tensile and flexural modulus. The composites with fibers provided the highest module, almost a twofold increase regarding the modulus of HDPE. This property appears to be more affected by the type of filler used than for the filler ratio, as no significant difference was found between 20% and 40% fiber or between 20% and 40% shredded material. However, the flexural modulus shows a different trend. In this case, the amount of filler is more significant than its type, finding similar values for 20% composites (again, with an improvement of 100% regarding the HDPE values). Finally, only composites with shredded materials do not show increased impact resistance, with 20% providing

Table 5. Average values (± standard deviations) for mechanical properties of the materials (for neat HDPE, the assay was stopped at 200% elongation prior to the breaking point of the samples).

	Impact	Tensile properties			Flexural properties		DMA		Hardness
Material	Strength [kJ/m^2 (Copani et al. 2013)	Strength [MPa]	Modulus [MPa]	ε_b [%]	Strength [MPa]	Modulus [MPa]	E′ [·10 (García-Ortuño et al. 2011)Pa]	B [·10 (Ferrández-García et al. 2012)Pa^{-1}%$^{-1}$]	Ball indentation hardness [MPa]
HDPE	6.37 ± 0.12^{a}	18.99 ± 0.07^{b}	1058 ± 16	>200*	26.54 ± 0.10	753 ± 56^{g}	1.402	<0.004	44.0 ± 0.5
PE.F20	7.47 ± 0.19	19.05 ± 0.11^{b}	$1881 \pm 45^{c,d}$	9.12	30.47 ± 0.23^{f}	1538 ± 77^{h}	1.734	0.633	52.0 ± 1.2
PE.F40	7.08 ± 0.14	17.46 ± 0.14	2022 ± 98^{c}	3.81	30.67 ± 0.22^{f}	1270 ± 125	1.928	1.361	59.6 ± 2.7
PE.S20	6.13 ± 0.13^{a}	19.05 ± 0.10^{b}	1560 ± 108^{e}	7.01	30.53 ± 0.22^{f}	1469 ± 23^{h}	1.659	0.860	49.9 ± 1.9
PE.S40	5.47 ± 0.18	16.36 ± 0.32	$1675 \pm 119^{d,e}$	2.70	28.98 ± 0.23	767 ± 73^{g}	1.782	2.081	57.3 ± 1.1

Tukey tests for comparison of properties of the different series of materials have been used at a 95% confidence level. Those materials with the same superscript letter show no statistical difference for the property.

similar behavior to PE, while 40% loadings reduce the impact strength. Composites with fibers exhibited an increase in impact strength of 17 and 11% for 20% and 40% fibers.

Other authors have reported that the incorporation of 12% of flax fiber has produced no changes in the tensile strength of a PE matrix and an increase of about 100% in elastic modulus; for flexural properties, this same composite provided an increase of about 75% flexural strength and almost doubled the flexural modulus and also led to a moderate increase, of about 10%, in impact strength (Bazan et al. 2020). Several works report a decrease in the mechanical performance of natural fiber composites and propose using compatibilizers, such as maleated polyethylene (MAPE), to increase the tensile strength of the resulting material (Jaramillo et al. 2021). For example, introducing MAPE in composites with 20% of hemp, jute, or flax provided similar or slightly higher tensile strength values than neat HDPE, 2-folding the elastic modulus (Dolza et al. 2021). The composites obtained with *Arundo*-derived materials have provided, in general terms, an improved mechanical behavior compared to the neat PE, already folding by two the elastic modulus of the polymer, thus demonstrating the good potential of these materials, particularly fibers, for composites obtaining; a similar trend was observed for bamboo fibers, which had a reinforcing effect for 20% loadings, increasing flexural strength and tensile and flexural modulus with increasing loadings of fibers, up to 30% (Mohanty and Nayak 2010). Mohanty and Nayak have also found a decrease in properties with further increases in the fiber content, which they relate to the incompatibility of fibers with the matrix; the incorporation of a 2% MAPE led to more significant improvements in mechanical properties, especially in modulus and flexural strength, which were improved by 100% in comparison to the composites at the same loading without the compatibilizer. In contrast, Lei et al. did not find any improvement by using MAPE or carboxylated polyethylene for 30% wood flour HDPE composites, which reduced tensile strength by over 30% and impact strength by more than 50% (Lei et al. 2007).

Table 5 also summarizes the results of ball indentation hardness of injection-molded polyethylene and its composites. The addition of both types of filler improved the hardness of the composites compared to neat HDPE. Taking into account the low tendency of HDPE to heterogeneous nucleation and the presented DSC results, it can be said that the effect of increasing the hardness results from the distribution of rigid filler structures in the boundary layer and not from a change in the degree of crystallinity of the polymer. Considering the changes in the chemical structure of *Arundo* fibers compared to shredded plant parts, the higher values of the series containing fibers are understandable.

A slight increase in hardness was found for composites. Neat HDPE exhibited a hardness of 60.0 Shore D, which increased to 62.5 for 20% composites and 65.0 for 40% composites. For this property, the ratio of filler is more significant than its type, as for the flexural testing. Similar values were obtained for 20% coir, flax, or coffee husks HDPE composites (Ayyanar et al. 2022; Chimeni-Yomeni et al. 0000; Jaramillo et al. 2021); lignocellulosic materials show a higher hardness than PE, which explains this trend.

Thermomechanical performance – DMA

The analysis of storage modulus (E′), loss modulus (E”), and damping factor (tanδ) with temperature allows evaluating the changes in the mechanical properties due to the addition of fibers and shredded material to the HDPE matrix (Figure 6). DMA is an essential test for the evaluation of the mechanical properties of materials due to its sensitiveness to to structural changes, including the interfacial bond between the fibers or fillers and the matrix (Correa-Aguirre et al. 2020).

The DMA storage moduli (Figure 6a) is indicative of the elastic behavior of the materials. All composites provide higher storage modulus than neat HDPE, meaning that the lignocellulosic material stiffens the matrix along the temperature range studied. The materials containing fibers show higher values of storage modulus than those made with shredded material, which means that these composites are stiffer, as also found in tensile and flexural tests. The starting value of the storage modulus is similar for all samples and tends to increase for composites while remaining constant for PE in the rubbery plateau area. The storage modulus decreases in an expected constant way, as also

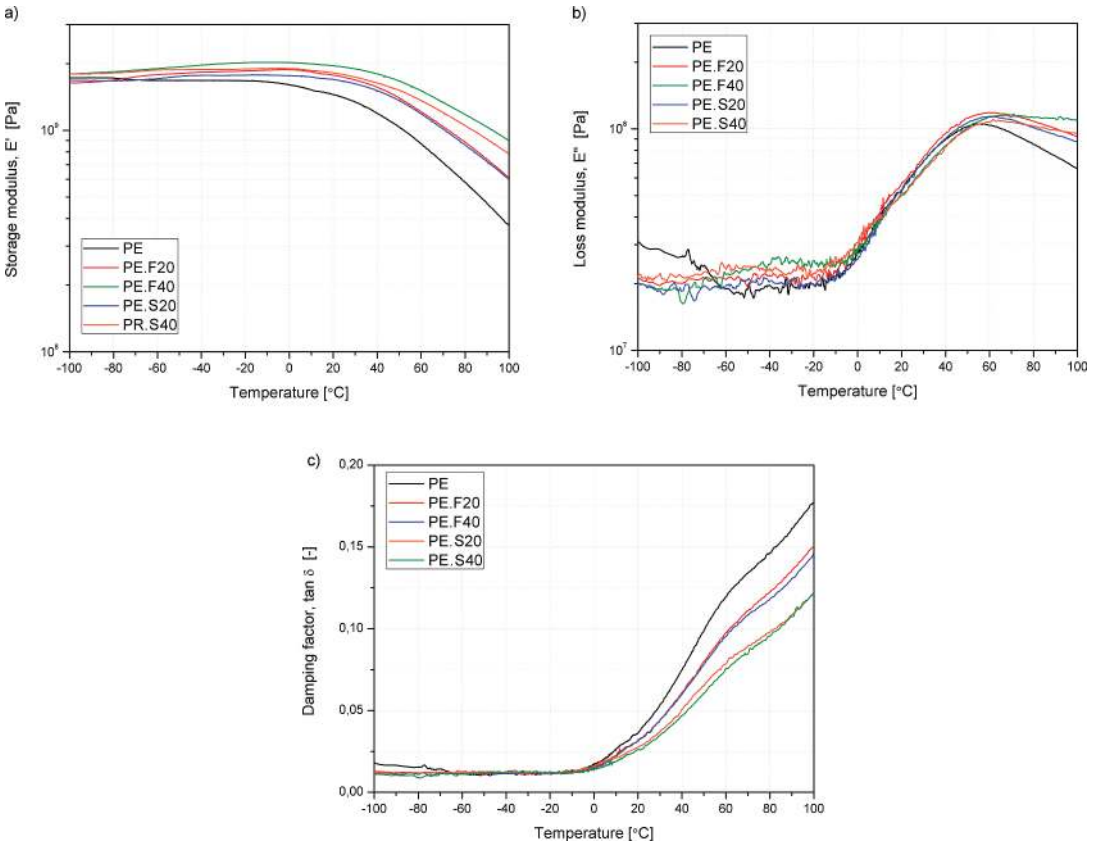


Figure 6. Variation of a) storage modulus, b) loss modulus and c) tan δ with temperature from DMA.

found in other works (Andrzejewski et al. 2020; Zhang et al. 2002). This decrease takes place at higher temperatures with the increase in lignocellulosic content.

The storage modulus for the HDPE decreased with temperature, while for composites there was a slight increase up to about 0°C, and then it started to decrease abruptly. HDPE composites with 20% microcellulose fibers, using 2% of MAPE as compatibilizer, led to an increase of 45% storage elastic modulus at −20°C (Fendler et al. 2007,) while for 20% hemp the increase reached 30% and 100%, again using MAPE as compatibilizer (Dolza et al. 2021,) at 0°C and 75°C. These authors have not provided results without the use of MAPE, so results are not directly comparable. Correo-Aguirre et al (Correa-Aguirre et al. 2020). observed an increase of 18% in storage modulus when using 20% of bagasse fibers in a PP matrix. The increased stiffness can be related to hindering HDPE polymer chain movements due to the introduction of fibers and shows that the composites have an increased capacity to store energy compared to the matrix. These results agree with the data obtained from impact tests, where higher values were also obtained for composites and are also observed in the reduced values of tan δ. For 20% *Arundo* fibers composite, the storage modulus increased by 11%, 16%, and 19% at −20°C, 0°C, and 75°C, and 21%, 25%, and 36% for 40% fibers. As observed in the graph, the shredded material also increases the storage modulus, although to lower values, namely 6, 9, and 17% for 20%, and 13, 17 and 29% for 40%, at the same temperatures.

For loss modulus, the PE maximum value is found at 57°C, corresponding to the α-transition, generally observed in the range from 20°C to 70°C (Molefi, Luyt, and Krupa 2010) or even 100°C (Hejna et al. 2020); this transition is related to chain movements in the crystalline region of the polymer. For the composites, this transition is slightly shifted to higher temperature values,

approaching 70°C for composites with 40% fibers. Composites with fibers show higher peak temperatures than shredded material. The shift of this transition toward higher temperatures and its increase indicates a more resistant structure in the composites and it is also related to the reduction in the polymer chain mobility. The β-transition for HDPE, usually related to segmental motions in the amorphous region, takes place at about 0°C; however, some authors have reported that this transition is usually absent (Mohanty and Nayak 2010,) as is also happening in this study.

Bhattacharjee and Bajwa (Bhattacharjee and Bajwa 2018) observed a 40% increase in storage modulus for HDPE loaded with wood flour, as well as an increase in tensile and flexural properties. The use of seaweed in a HDPE leads to an increase of the storage modulus of about 10%, which increases with the seaweeds content, up to 30% (Ferrero et al. 2015). The introduction of 30% of banana fiber in HDPE, with a 3% of MAPE as compatibilizer, leads to similar results: around 30% increase in storage modulus, maximum temperature from E" plot shift from 57°C to 63°C and a slight decrease in tan δ (0.18 to 0.16) (Satapathy and Kothapalli 2018). Lei et al. found an increase in both storage and loss modulus when using bagasse or pine flour in a recycled HDPE matrix, for a 30% loading (Lei et al. 2007). At 23°C, storage modulus increased from 1.55 GPa for HDPE to 2.29 GPa and 2.23 GPa for bagasse and pine, respectively, while loss modulus varied from the initial 0.15 GPa to 0.19 and 0.18 GPa, respectively. These authors did not get further improvements by using compatibilizers such as MAPE or carboxylated polyethylene. All *Arundo* composites show lower loss modulus than pure PE, which means that the incorporation of the lignocellulosic materials provides higher elastic recovery. γ-transitions occur for HDPE at temperatures lower than the ones used in the study, and so are not visible, although they might correspond to the small peak seen around −70°C (Molefi, Luyt, and Krupa 2010,) also visible in storage modulus as a short descending step for PE.

The glass transition temperature (T_g) in highly crystalline polymers, as it is the case of HDPE, is difficult to identify; this is in line with the results obtained in this research. The glass transition occurs when the chains in the amorphous regions begin a coordinated large-scale motion. Therefore, this transition is not observable in the highly crystalline HDPE, although an intense peak for α-transition is usually observed. DSC has provided crystallinity values over 45% for all samples, reaching up to 60%, which may explain that T_g is not visible in these assays, so the plots do not show this characteristic peak. The tan δ plot shows an inflection in the curves at 50–60°C, corresponding to α-transition, also observed in E" plots as a maximum.

The tan δ is the ratio of the loss to the storage modules; therefore, the damping factor is useful to assess the relative contributions of the viscous and elastic components in viscoelastic materials. Again this curve does not show the β-transition, although a slight inflexion in the curves is seen at about 10°C; this could be attributed to the glass-rubber transition of the amorphous phase (Barczewski et al. 2018). The increased stiffness found for composites implies a reduction in damping properties, compared to the neat PE, as seen from the tan δ plot. The composites with higher stiffness revealed lower values of damping factor, as also observed by other authors (Barczewski et al. 2018). The thermomechanical behavior of the materials is apparently more influenced by the amount of lignocellulosic material than by its type. Good fiber-matrix adhesion limits the mobility of polymer chains and thus reduce the damping factor, with a simultaneous increase of T_g (Scalici, Fiore, and Valenza 2016); obtained results would then suggest that fibers are well bonded to the matrix.

From the DMA results the brittleness (B) of the different materials can be calculated, using equation 8, proposed by Brostow et al (Brostow, Hagg Lobland, and Khoja 2015):

$$B = \frac{1}{\varepsilon_b \cdot E'} \tag{10}$$

Where E' is the storage modulus from DMA at 1.0 Hz and ε_b the elongation at break, both at room temperature.

The brittleness values obtained at 25°C for the different formulations are found in Table 5. According to these authors, lower brittleness values imply higher dimensional stability of the

material under repetitive loading. So, 20% composites would be more stable than 40% ones, and fibers are more stable than shredded material. Another factor that can be calculated from DMA analysis is the adhesion factor (A in equation 9), as described by Kubat et al (Kubát, Rigdahl, and Welander 1990,) and considering that the behavior of the composite is due to the properties of the matrix, the filler and the interphase, and resulting in (Hejna et al. 2020):

$$A = \frac{1}{1 - x_F} \cdot \frac{tan\delta_C}{tan\delta_{PE}} - 1 \tag{11}$$

Where x_F is the ratio of the filler in the composite (in volume).

Lower values of A indicate higher interfacial adhesion (Jyoti et al. 2016); an increase in A is associated with higher damping and a higher loss of energy or viscoelastic behavior, and higher energy dissipation due to chain movements inside the composite (Karaduman et al. 2014). Hejna et al (Hejna et al. 2020). explain that a high porosity or insufficient interfacial adhesion favors these movements. As this factor depends on the damping factor, it also varies with temperature. It can be seen that at higher loadings, higher values of the adhesion factor are observed, and therefore there is lower adherence between the lignocellulosic material and the matrix. The values for this parameter are similar regardless of the type of lignocellulosic material introduced. The negative values of the adhesion factor obtained are due to the simplification of the calculations and the removal of the interphase region (Hejna et al. 2020; Mysiukiewicz et al. 2020). The lower and more stable values are obtained at temperatures over 15°C, meaning that the lignocellulosic materials do not provide as much positive effect below room temperature.

Several authors propose using the entanglement factor as an approximation to the intensity of the interaction between matrix and filler/reinforcement, together with the efficiency factor (Andrzejewski et al. 2020; Jyoti et al. 2016; Pandey et al. 2016; Panwar and Pal 2017). The entanglement factor is usually calculated at several temperatures to evaluate the potential differences in such interactions due to different service conditions. The entanglement factor (N) is calculated as:

$$N = \frac{E'}{RT} \tag{12}$$

Where E' is the storage modulus at a certain temperature (T, in K) and R is the universal gas constant.

The reinforcement efficiency (r) also gives an idea of the filler/matrix interaction:

$$E'_c = E'_m \cdot \left(1 + r \cdot V_f\right) \tag{13}$$

Where E'_c and E'_m are the storage modulus of the composite and the matrix, respectively, and V_f the percentage of the filler (by volume).

It is interesting to note that lower values of the entanglement factor are found for 20% composites up to approximately −70°C, possibly corresponding to the end of γ-transition of the HDPE (Khanna et al. 1985) (Figure 7b). From that moment, the difference in storage modulus is increasing with the temperature, getting the lowest value for the neat HDPE. A clear difference between the composites with fibers and with shredded material is observed for this factor, as also found in tensile and flexural tests. The efficiency factor increases abruptly after approximately 15°C. This was also observed in the storage modulus versus temperature plot, where the composites provided higher values of E' than the neat HDPE. These findings are in good agreement with the static mechanical results, where higher mechanical performance was obtained for fibers, particularly at 20%.

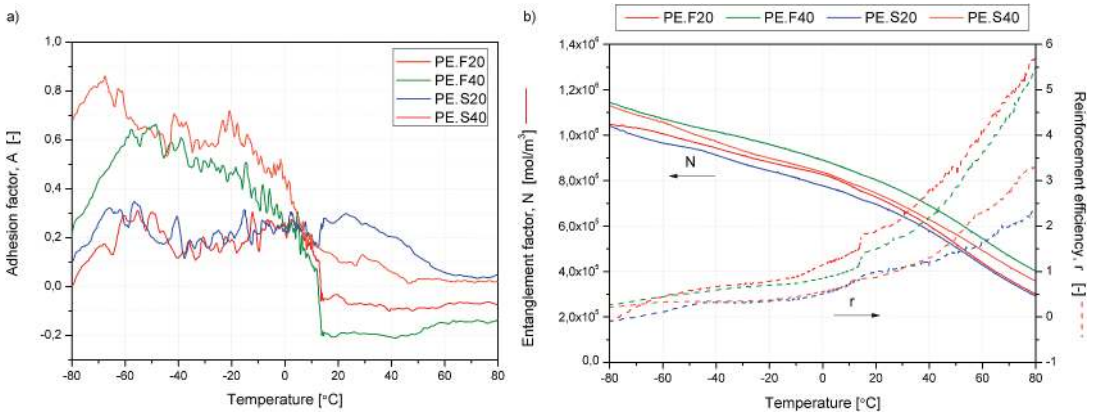


Figure 7. a) adhesion factor calculated for the composites, b) entanglement factor (left axis) and reinforcement efficiency (right axis).

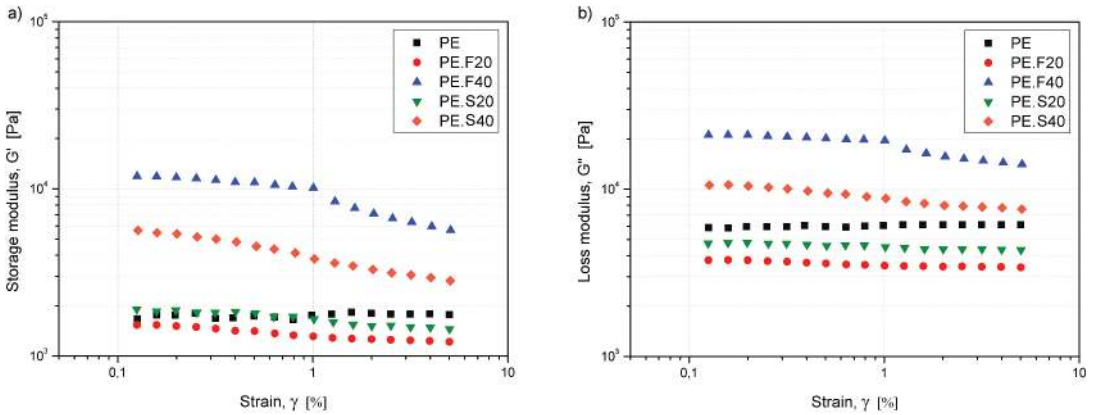


Figure 8. Results of strain-sweep rheological experiments: a) storage modulus, b) loss modulus.

Rheological behavior

Oscillatory rheometry

Figure 8 shows the storage and loss modulus (G' and G") versus strain (γ), obtained during strain sweep assays. It can be observed that the introduction of 20% lignocellulosic filler of both types to HDPE does not cause significant modifications of the storage and loss moduli, while both increase for 40% composites. HDPE and composites at 20% exhibit a similar trend, with a linear viscoelastic (LVE) region in the studied range (0.1–5% strain), while 40% loadings show a shorter LVE area, with a short step around 1% strain, although this is not considered particularly significant. The frequency sweep tests were performed at 0.5% strain, thus in the LVE for all materials. It is well known that incorporating fillers into polymer matrices usually produces a shortening of this LVE region; this is connected with the creation of the spatial structure of restricted rigid filler domains (Adebayo et al. 2021; Berzin et al. 2019). 0.5% strain is a commonly used value for PE-based materials and oscillation mode assays. For this strain, the value of G' for HDPE is 1.7 kPa, similar to 20% composites as observed in the graph (1.4 and 1.8 kPa for fibers and shredded material, respectively), while this increased significantly for 40% composites, increasing by almost 300% for shredded material (reaching up to 4.5 kPa) and by 800% for fibers (arriving almost to 11 kPa).

Figure 9 shows, in logarithmic scale, the results of frequency sweep tests, in the oscillation mode, versus angular frequency (ω). At lower ω all composites provide higher values of both moduli than the

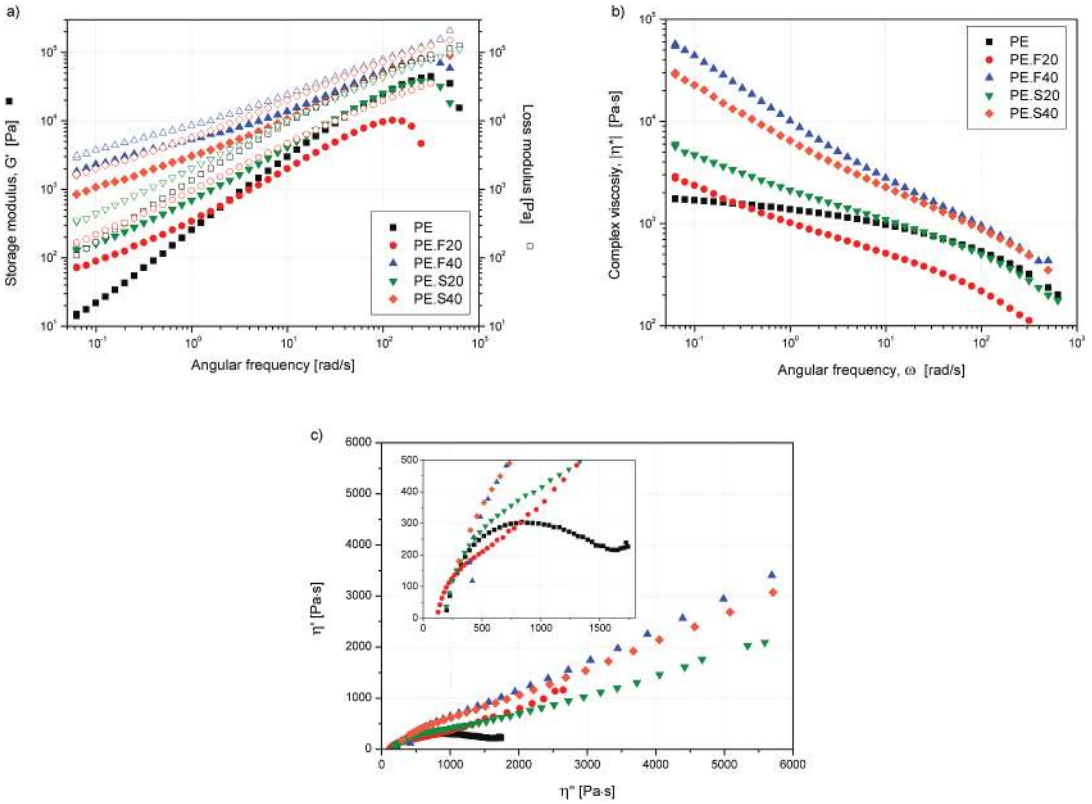


Figure 9. Results of frequency-sweep rheological experiments: a) storage and loss modulus, b) complex viscosity, c) Cole-Cole plot.

neat polyethylene, although at higher frequencies, the trend changes, and only 40% loadings show higher moduli than PE, as observed by Patti et al. for PP composites (Patti et al. 2021). The values of G" are higher than those of G' for all composites, which means the viscous part is dominant over all of the studied range; both curves follow a linear trend in a similar pattern for each material. The increase in moduli is evident in the low-frequency range (0.1–10 rad/s), as the curves tend to overlap at high frequencies, likely due to the fibers aligning at higher frequencies.

No flow point is obtained for any of the composite materials with 40% loadings, that is, the storage and loss modulus do not cross-over each other in the studied region. The increase of both modules shows the reinforcing effect of the lignocellulosic materials, with a predominant viscous character of the rheological behavior. This effect suggests that the obtained composites materials, despite the higher resistance to flow of the filled bulk, will not be characterized with limited processability.

Figure 9b shows the complex viscosity ($|\eta^*|$) for the materials tested. A Newtonian plateau is observed for neat HDPE at frequencies under 10 rad/s, which does not occur for composites, which are more shear thinning in nature, as observed in other works also (Hejna et al. 2020). Complex viscosity is higher for the 40% composites, but is reduced for 20% fiber composites, especially for shear rates over 1 rad/s. The use of shredded material at this loading only increases the viscosity at low ω values, which would again suggest fiber alignment and overlapping at high ω. The lack of plateau observed for composites could indicate the formation of agglomerates of the lignocellulosic materials in the samples (Barczewski et al. 2022; Berzin et al. 2019). The greater viscosity increase in low ω range results from increased physical impact of the fibrous *Arundo* filler characterized with higher aspect ratio. Other works have shown a moderate increase of viscosity for up to 30% loadings of wood-derived materials, with abrupt increases for 40% composites, which result in a more difficult processing of such

composites (Adebayo et al. 2021; Koohestani et al. 2019). The viscosity curves for all materials show shear thinning behavior or pseudoplasticity, meaning they become less viscous at increasing angular frequencies. As also found in the literature, at high frequencies the effect of the interaction between particles becomes less prominent than the matrix contributions and thus the viscosity values for composites tend to approach that of the matrix (Adebayo et al. 2021; Ogah, Afiukwa, and Nduji 2014).

The real and imaginary parts of the complex viscosity allow the evaluation of the compatibility of polymer blends or composite materials (Aid et al. 2019; Mysiukiewicz et al. 2020). This method, known as Cole-Cole plot (Figure 8c), states that miscible homogeneous blends provide semi-circle-shaped smooth curves, while deviations from this Maxwellian fluid ideality reflect a poor distribution or miscibility of the phases studied. For this study, it is seen that PE has a relatively smooth course, close to a semicircle, as also do 20% composites, at least to a certain value. Forty percent composites show a higher deviation from the ideal plot, especially at higher viscosity values, where the curves tend to form a straight line, thus indicating agglomerations of the filler, as found in other works (Mysiukiewicz et al. 2020; Stanciu et al. 2020).

Finally, the flow tests were performed to determine the zero-shear viscosity (η_0), using the Carreau-Yasuda regression. As for all the parameters studied, the values for η_0 increase with the biomass loading, i.e. 1579 Pa·s (PE), 2529 Pa·s (PE.F20), 37970 Pa·s (PE.F40), 5156 Pa·s (PE.S20), 13250 Pa·s (PE.S40). Those results are in agreement with the MFI values and with data reported in the literature (Adebayo et al. 2021; Berzin et al. 2019; Mohanty and Nayak 2010) and with the increases recorded in switchover pressure during injection molding: the higher lignocellulose content resulted in lower MFI, or higher viscosity of the material (Figure 9). The composites with shredded material have a higher viscosity and lower density than those with fibers. Figure 10 shows the mean MFI values obtained for the different materials, and the modification of zero-shear stress and switch pressure during processing compared to the values obtained for neat HDPE.

Capillary rheometry

The effect of two different lignocellulosic fillers incorporated with 20% and 40% on rheological behavior during capillary flow was additionally investigated. The results are presented as changes of shear viscosity (η) in the function of apparent shear rate (γ_A) in Figure 11. The addition of the filler increased the shear

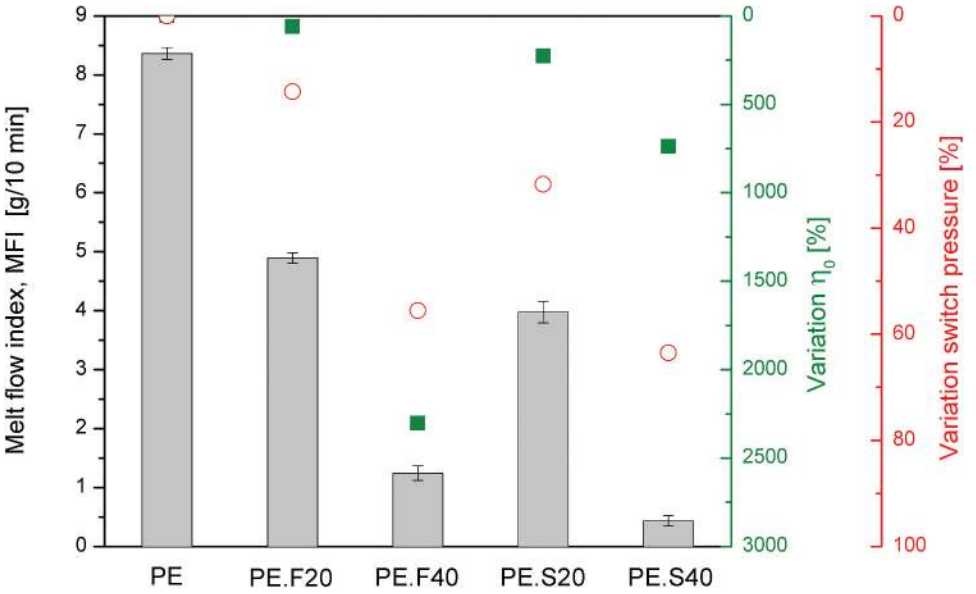


Figure 10. MFI and variation of zero-shear stress and switchover pressure for the different materials.

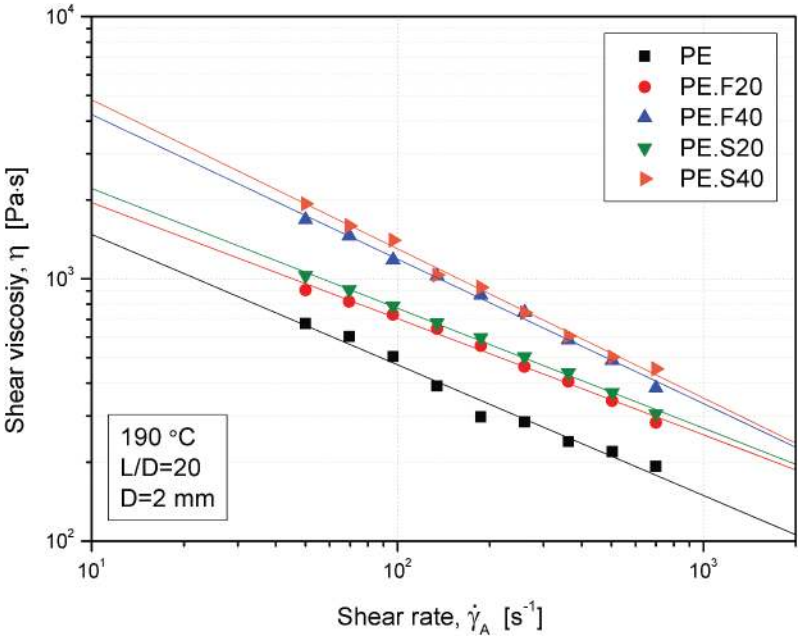


Figure 11. Shear viscosity vs. shear rate curves obtained by capillary rheology.

viscosity compared to unmodified polyethylene. This phenomenon is characteristic of polymer composites and was also noted for other materials modified with lignocellulosic fillers (Kuan et al. 2003; Lewandowski et al. 2016). *Arundo* fiber composites were characterized by slightly lower viscosities compared to shredded-filled series, as was also observed in oscillatory tests. The slight differences most likely resulted from the tendency of the fibrous material to orient in the flow direction during capillary flow, which resulted in a lower flow resistance than for composites filled with irregularly particle-shaped filler with a low aspect ratio.

The determination of the power law index (n) according to Equation (8), allows to describe the nature of fluid as Newtonian (n = 1), non-Newtonian shear-thinning (0 < 1), or shear thickening (n > 1) (Smitthipong, Tantatherdtam, and Chollakup 2015). The analyzed composites show, similarly to the unmodified polymer, shear-thinning behavior. The decrease in the value of the power law index noted for series with the highest share of filler in polymeric bulk is typical to the behavior of polymer composites (Ares et al. 2010,) as described in the literature. In the case of the unmodified high-density polyethylene, the *n* value is lower than for composites containing 20 wt% of the filler. This effect is rather not due to a change in the non-Newtonian nature of the flow but to the higher likeness of non-filled high-density polyethylene to the stick-slip phenomenon (Barczewski et al. 2017,) which results in a lower degree of fitting of the model curve to experimental data, as shown in Table 6. The consistency factor K increased with the filler content, resulting from increased resistance to the flow of polymeric melts with dispersed rigid lignocellulosic structures (Sewda and Maiti 2010). Moreover, this parameter is higher for composites containing shredded

Table 6. Power law model parameters for PE and PE composites.

Material	K [Pa·s^n]	n [-]	R^2 [-]
PE	4,654	0.502	0.981
PE.F20	5,420	0.557	0.989
PE.F40	15,035	0.449	0.996
PE.S20	6,328	0.543	0.997
PE.S40	17,867	0.431	0.994

Arundo than for those with the fibrous filler; the explanation for this phenomenon may be the increased interaction between the irregularly shaped filler particles during the capillary flow and the increased interaction behavior of its constituents.

Structure evaluation

Figure 12 shows a representative image from SEM observation of the test samples surface for each formulation. The surface for neat HDPE is smooth and without marks, while the composites show a rougher surface, with some lignocellulosic material close to the surface, leading to flow marks and shrinks. As explained in section 3.9, this different roughness explains the changes in gloss observed for composites versus the pure matrix.

From the fracture section of the samples after the tensile tests, it can be observed (Figure 13) that fibers are not aligned in a particular direction but are rather found well dispersed in the matrix, without any preferent orientation. On the other hand, some pull-out can be seen, more relevant for the composites at higher loadings. For the same ratio of filler, more pull-out was found for materials with shredded reed. This is in agreement with the observation on the adhesion factor and the reinforcing efficiency; fibrous composites show better adhesion and higher efficiency than those with shredded lignocellulose materials, also explaining the better mechanical performance of such series of materials.

In Figure 13a SEM images, the cross-sections of samples with 20% and 40% fiber can be observed. In the 20% one, no signs of evident pull-out are observed, while this is evident for the 40% composite, where some voids appear as a consequence of insufficient adhesion between fiber and matrix. The slight reduction in tensile strength found for this series of composites (regarding neat HDPE) might be explained by the debonding of part of the fibers. On the other hand, Figure 13c shows a section of a PE. F20 sample at a higher magnification, where it is patterning that all fibers are not strongly bonded to the matrix. Although an increase in elastic modulus is found for composites, the good stress transfer between fiber and matrix (requiring a good adhesion between phases) is evidenced by the increase in tensile strength, which wasn't obtained for these composites and is also happening in the literature. Some compatibilizers would be needed to increase the compatibility between both phases; however, special attention should be paid to the selection and application of such treatment. Most of them focus on the use of coupling agents, such as maleated polyethylene; not all authors have found

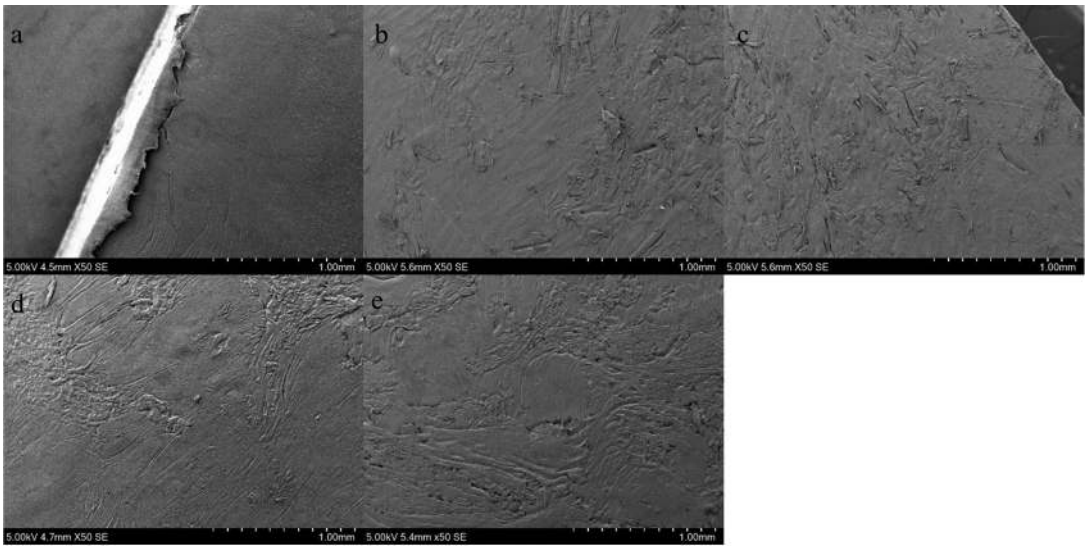


Figure 12. SEM images of the surface of the different parts, obtained at 50× magnification: a) PE, b) PE.F20, c) PE.F40, d) PE.R20, e) PE.R40.

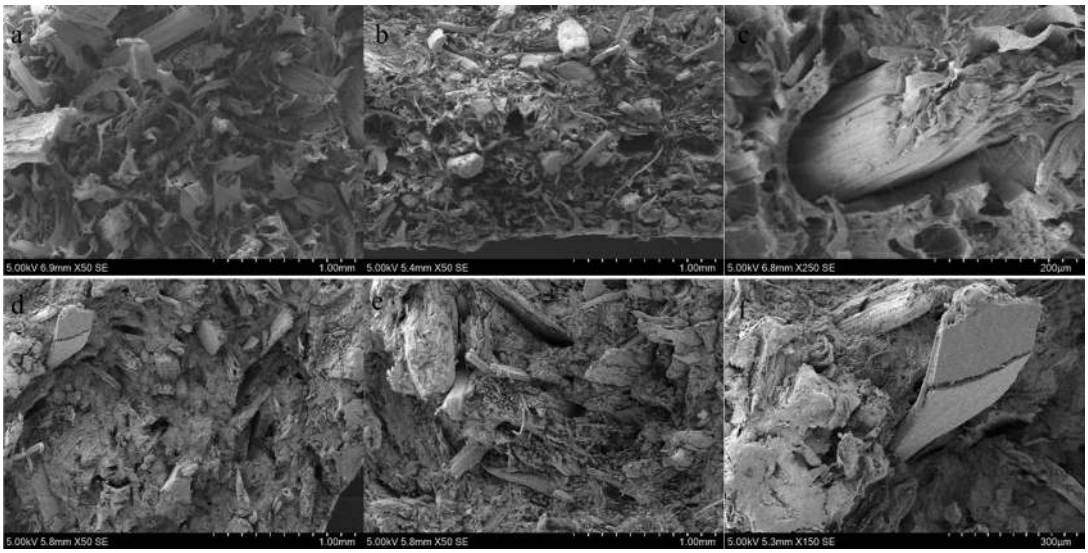


Figure 13. Cross-section micrographies for the different parts, obtained at different magnifications: a) PE.F20 and b) PE.F40 at 50×, c) PE.F20 at 250×; d) PE.R20 and e) PE.R40 at 50×, f) PE.R20 at 150×).

improvements in mechanical performance, despite the expected better adhesion, as explained in sections 3.5 and 3.6. Similar observations are made for silanized fillers, this last releasing an important amount of volatile compounds. A balance between technical performance of the composite and environmental behavior should be reached. Similar observations can be made regarding the composites with shredded materials, although finding, in this case, a higher number of voids (Figure 13d,e); that is, the adhesion between the HDPE matrix and the filler is lower than for the case of fibers, which is in line with the observations made from static and dynamic mechanical testing. Finally, it is also evidenced for these composites that the filler consists of less homogeneous materials, with fibers and fiber bundles (Figure 13f).

Color and gloss evaluation

The results from color and gloss evaluation are summarized in Table 7. The decrease in the L* parameter is related to the darkening of the samples. From these values, and as observed in Figure 14, composites with fiber are lighter and tend more yellow than those with shredded material, which are darker and greener. Despite the different values for the L*, a*, and b* parameters obtained for all composites, the color changes in the neat PE are similar for all samples. Regarding gloss, it can be observed that fiber composites at both loadings provide a matted surface with lower gloss than composites with shredded materials. At the same time, the gloss of composite shredded materials decreased with the increased content of filler. The lower gloss is due to the rougher surface obtained for composites.

Table 7. Parameters for color and gloss evaluation.

	Color				Gloss		
Material	L*	a*	b*	ΔE	20º	60º	85º
PE	72.47 ± 0.13	−0.91 ± 0.03	−0.31 ± 0.12	–	27.38 ± 3.46	69.03 ± 5.06	84.72 ± 2.17
PE.F20	56.26 ± 0.86	12.37 ± 0.45	23.67 ± 0.91	31.845	0.98 ± 0.17	7.83 ± 1.12	8.46 ± 2.74
PE.F40	58.37 ± 1.34	12.00 ± 0.69	26.16 ± 1.37	32.651	1.06 ± 0.54	7.63 ± 2.93	17.42 ± 5.51
PE.S20	41.61 ± 1.24	5.32 ± 0.30	18.77 ± 0.62	36.810	7.13 ± 0.99	32.39 ± 3.15	53.89 ± 2.91
PE.S40	49.33 ± 1.48	4.44 ± 0.24	15.61 ± 1.00	28.593	3.01 ± 0.95	18.16 ± 4.21	35.51 ± 7.33

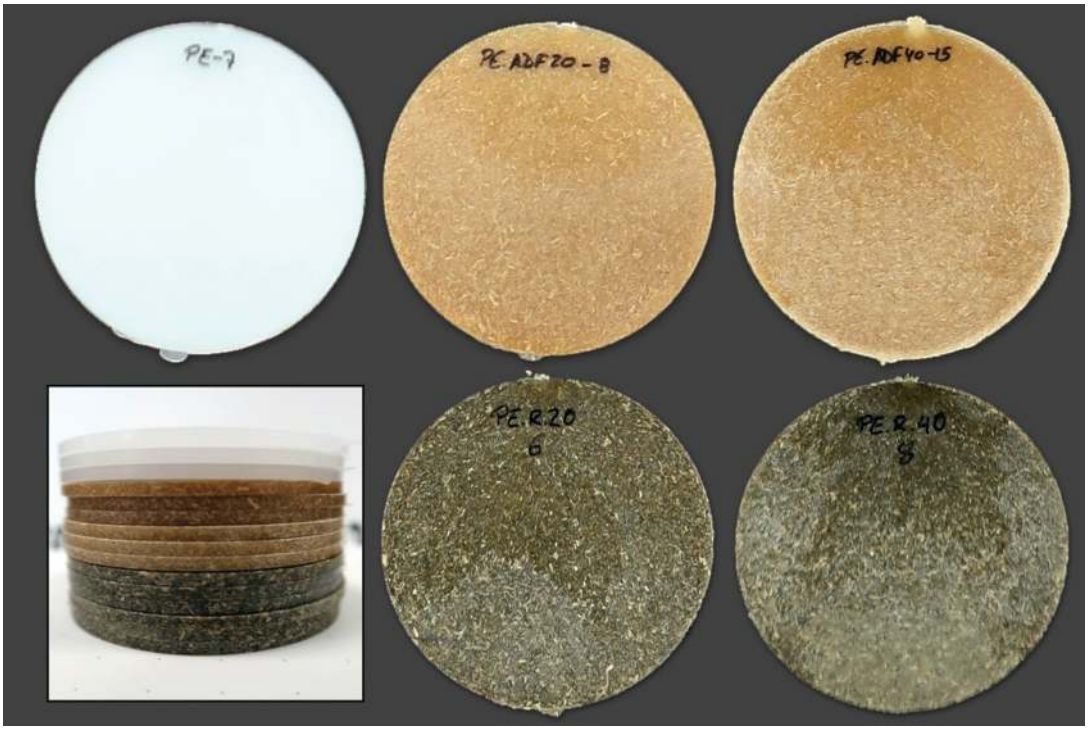


Figure 14. Photography of injection-molded samples of the various formulations.

Conclusions

The obtaining of composite materials containing giant reed is still rather incipient in the literature, contrary to other lignocellulose fibers, or to other uses given to this plant species. Most literature about *Arundo donax* L. is related to the obtaining of green products, such as ethanol or levulinic acid. In this work, two different *Arundo donax* L. derived materials have been used for obtaining composites at 20% and 40% weight loadings, obtaining a material with a good processability window (higher degradation temperature than the processing one required: degradation starts at 240°C, which is 50°C above the processing temperature).

The viscosity of the composites increases with the amount of filler used, finding a more viscous material for the composites with the fibrous material in contrast to the shredded material, due to the higher aspect ratio of the filler. The increased viscosity is well correlated with the reductions in MFI and the higher values of switch over pressure during the injection molding of the composites.

The FTIR analysis does not evidence any particular chemical interaction between filler and matrix; the formation of chemical bonds between both phases would require a compatibilizer and might reduce the pull-out of fibers in the mechanical testing, thus, to higher mechanical properties.

In any case, a good stress transfer is observed for the composites, particularly for those containing reed in the form of fibers, even though any compatibilizer was introduced in the process. The tensile and flexural strength was not reduced, and elastic modules in both assays were increased significantly. So, composites with 20% fiber exhibit a tensile strength of about 19 MPa and an elastic modulus of 1.9 GPa, which is almost twice that of the neat matrix, while flexural strength of this series is increased by a 15% (reaching 30 MPa) and elastic modulus is also increase by over 100%, getting over 1500 MPa. The increased porosity found for composites has not reduced the mechanical properties of the composite, which is a further indicator of the good behavior of the *Arundo*-derived materials in the HDPE matrix. In any case, porosity values

are considered low, finding the maximum value of 8.7% for 40% fiber composites; this can be related to a good processing of the materials and also to the good thermal stability of the material: as it is not degraded during processing, no decomposition products, in the form of vapor or gases, are generated. Finally, only those composites with fiber increased the impact resistance of the matrix, which might be related to better adhesion of the fiber to the matrix, as also found in SEM observations and DMA assays. Impact strength is increased by 20% for fibrous composites, while the composites with 20% shredded material provided comparable values to the HDPE; only the series with 40% shredded material shows a slight decrease of about 10% for this property.

The TGA assays have allowed confirming that the ratio of each filler used corresponds to the blend prepared at the compounding stage, apart from confirming that the material is thermally stable for about 50°C above the required processing temperature. Neither the melting point nor the crystallinity of the matrix is affected by incorporating the lignocellulose materials, as commonly accepted in literature for HDPE-based composites; melting takes place at about 135°C. However, the heat deflection and Vicat softening temperatures are significantly increased as a consequence of biomass incorporation; in particular, HDT is almost increased by 100% for the 40% fiber composites (41°C for neat HDPE vs. 73°C for this composite), while VST rises from 72°C for the matrix to 86°C for this same material. This increase might be an indicator of the good stability of injection-molded composites for their use under temperature-changing conditions, such as outdoor applications. In any case, the aging performance and stability of such materials under UV and humidity cycles should be assessed prior to anticipating a good behavior under such circumstances. The content of polyphenols and other antioxidant compounds in biomass would provide additional benefits to consider. These tests, together with the analysis of recyclability and the study of lifecycle of composites would allow establishing the techno-environmental benefits of using such materials in contrast to the neat matrix or to other composites obtained with natural fibers. The use of a lignocellulosic filler coming from a residue would *a priori* result in an improved environmental behavior, although this point is being confirmed in the near future by conducting a proper LCA.

Despite their different composition, a significant increase in water uptake for the composites was observed, without significant differences due to the type of filler. Swelling is more significant for the composites with higher loading, reaching values up to 8% for PE.F40 samples. The values obtained for diffusion coefficients are similar to those obtained in literature for other composites with lignocellulose fibers, in the range of $2.3–3.6{\cdot}10^{-13}$ m (Copani et al. 2013)/s, in the range of 100 times higher than for neat HDPE polymer, of hydrophobic nature.

Finally, introducing the biomass in the HDPE matrix results in changes in the aesthetics of the part; while composites with fibers tend to get a yellowish color, those with shredded reeds show a greener aspect. The different flow behavior of both composites explains the higher surface roughness observed in SEM for the fiber composites, which results in a matte appearance, regardless of the fiber ratio used. For the composites with 20% of the shredded material, a thin layer of PE is likely to be formed on the outer surface of the part, producing a smoother surface with higher gloss, which is also reduced for the higher-loaded samples.

Therefore, the potential of giant reed as raw material to produce fibers and fillers has been demonstrated, allowing to obtain a composite with good aesthetics, thermal stability, and mechanical performance. Further experiments are being conducted to determine other properties of the composites and finish their characterization; in particular, the resistance to oxidation/aging under humid environment and UV light, the thermal and acoustic insulating character, and the environmental behavior, including an analysis of the recyclability of the material, are being undertaken.

Highlights

- HDPE-based composites with up to 40% biomass from *Arundo donax* were produced.
- Addition of 20 wt% *Arundo* improve elastic and flexural modulus.
- Thermal stability is increased due to the incorporation of *Arundo* biomass.
- Fibrous filler provided better adhesion and properties than particle-shaped one.

Acknowledgments

Luis Suárez: Ph.D. grant program co-financed by the Canarian Agency for Research, Innovation and Information Society of the Canary Islands Regional Council for Employment, Industry, Commerce and Knowledge (ACIISI) and by the European Social Fund (ESF) (Grant number TESIS2021010008).

Disclosure statement

No potential conflict of interest was reported by the author(s).

Funding

The work was supported by the Agencia Canaria de Investigación, Innovación y Sociedad de la Información [TESIS2021010008]; Spanish Ministry of Universities [Next Generation funds (Order UNI/501/2021)].

ORCID

Luis Suárez http://orcid.org/0000-0002-6709-1555
Zaida Ortega http://orcid.org/0000-0002-7112-1067
Mateusz Barczewski http://orcid.org/0000-0003-1451-6430
Paulina Kosmela http://orcid.org/0000-0003-4158-2679
Bronagh Millar http://orcid.org/0000-0003-3961-0087
Eoin Cunningham http://orcid.org/0000-0003-2555-7705

Author contributions

Conceptualization: Zaida Ortega; Methodology: Zaida Ortega, Luis Suárez, Mateusz Barczewski, Paul R. Hanna; Formal analysis: Luis Suárez, Paul R. Hanna, Zaida Ortega, Mateusz Barczewski, Paulina Kosmela, Bronagh Millar, Eoin Cunningham; Investigation: Luis Suárez, Paul R. Hanna, Zaida Ortega, Mateusz Barczewski, Paulina Kosmela, Bronagh Millar, Eoin Cunningham; Supervision: Zaida Ortega; Visualization: Luis Suárez, Mateusz Barczewski; Writing – original draft: Luis Suárez, Zaida Ortega, Mateusz Barczweski; Writing – review & editing: all authors.

References

Adebayo, G. O., A. Hassan, R. Yahya, F. Okieimen, and N. M. Sarih. 2021. "Dynamic Rheological Properties of Spotted Mangrove/high-Density Polyethylene Composites." *Journal of Thermoplastic Composite Materials* 34 (9): 1273–1285. https://doi.org/10.1177/0892705719870587.

Aid, S., A. Eddhahak, S. Khelladi, Z. Ortega, S. Chaabani, and A. Tcharkhtchi. 2019. "On the Miscibility of PVDF/PMMA Polymer Blends: Thermodynamics, Experimental and Numerical Investigations." *Polymer Testing* 73:222–231. https://doi.org/10.1016/j.polymertesting.2018.11.036.

Andreu-Rodriguez, J., E. Medina, M. T. Ferrandez-Garcia, M. Ferrandez-Villena, C. E. Ferrandez-Garcia, C. Paredes, M. A. Bustamante, et al. 2013. "Agricultural and Industrial Valorization of Arundo donax L." *Communications in Soil Science and Plant Analysis* 44 (1–4): 598–609. https://doi.org/10.1080/00103624.2013.745363.

Andrzejewski, J., B. Gapiński, A. Islam, and M. Szostak. 2020. "The Influence of the Hybridization Process on the Mechanical and Thermal Properties of Polyoxymethylene (POM) Composites with the Use of a Novel Sustainable Reinforcing System Based on Biocarbon and Basalt Fiber (BC/BF)." *Materials* 13 (16): 3496. https://doi.org/10.3390/MA13163496.

Andrzejewski, J., A. Krawczak, K. Wesoły, and M. Szostak. 2020. "Rotational Molding of Biocomposites with Addition of Buckwheat Husk Filler. Structure-Property Correlation Assessment for Materials Based on Polyethylene (PE) and Poly(lactic Acid) PLA." *Composites Part B Engineering* 202:108410. https://doi.org/10.1016/j.compositesb.2020.108410.

Ares, A. R. Bouza, S. G. Pardo, M. J. Abad, and L. Barral 2010. "'Rheological, Mechanical and Thermal Behaviour of Wood Polymer Composites Based on Recycled Polypropylene'." *Journal of Polymers and the Environment* 18: 318–325. doi:10.1007/s10924-010-0208-x.

Ayyanar, C. B., M. D. Dharshinii, K. Marimuthu, S. Akhil, T. Mugilan, C. Bharathiraj, S. Mavinkere Rangappa, et al. 2022. "Design, Fabrication, and Characterization of Natural Fillers Loaded HDPE Composites for Domestic Applications." *Polymer Composites* 43 (8): 5168–5178. https://doi.org/10.1002/pc.26806.

Balasuriya, P. W., L. Ye, and Y. W. Mai. 2003. "Morphology and Mechanical Properties of Reconstituted Wood Board Waste-Polyethylene Composites." *Composite Interfaces* 10 (2/3): 319–341. https://doi.org/10.1163/156855403765826946.

Baquero Basto, D., J. Monsalve Alarcón, and M. Sánchez Cruz. 2018. "Experimental Characterization of Composite Panels Made with Arundo Dónax Fibers and Vegetable Resin." *Sciencia et Technica* 23:119–125. https://www.redalyc.org/journal/849/84956661017/84956661017.pdf.

Barana, D., A. Salanti, M. Orlandi, D. S. Ali, and L. Zoia. 2016. "Biorefinery Process for the Simultaneous Recovery of Lignin, Hemicelluloses, Cellulose Nanocrystals and Silica from Rice Husk and Arundo Donax." *Industrial Crops and Products* 86:31–39. https://doi.org/10.1016/j.indcrop.2016.03.029.

Barczewski, M., A. Hejna, J. Aniśko, J. Andrzejewski, A. Piasecki, O. Mysiukiewicz, M. Bąk, et al. 2022. "Rotational Molding of Polylactide (PLA) Composites Filled with Copper Slag as a Waste Filler from Metallurgical Industry." *Polymer Testing* 106:107449. https://doi.org/10.1016/J.POLYMERTESTING.2021.107449.

Barczewski, M., K. Lewandowski, M. Schmidt, and M. Szostak. 2017. "Melt fracture and rheology of linear low density polyethylene - calcium carbonate composites." *Polymer Engineering & Science* 57 (9): 998–1004. https://doi.org/10.1002/pen.24477.

Barczewski, M., D. Matykiewicz, O. Mysiukiewicz, and P. MacIejewski. 2018. "Evaluation of Polypropylene Hybrid Composites Containing Glass Fiber and Basalt Powder." *Journal of Polymer Engineering* 38 (3): 281–289. https://doi.org/10.1515/polyeng-2017-0019.

Barreca, F., A. Martinez Gabarron, J. A. Flores Yepes, and J. J. Pastor Pérez. 2019. "Innovative Use of Giant Reed and Cork Residues for Panels of Buildings in Mediterranean Area." *Resources, Conservation and Recycling* 140:259–266. https://doi.org/10.1016/J.RESCONREC.2018.10.005.

Bazan, P., D. Mierzwiński, R. Bogucki, and S. Kuciel. 2020. "Bio-Based Polyethylene Composites with Natural Fiber: Mechanical, Thermal, and Ageing Properties." *Materials* 13 (11): 2595. https://doi.org/10.3390/ma13112595.

Berzin, F., T. Amornsakchai, A. Lemaitre, R. Castellani, and B. Vergnes. 2019. "Influence of Fiber Content on Rheological and Mechanical Properties of Pineapple Leaf Fibers-Polypropylene Composites Prepared by Twin-Screw Extrusion." *Polymer Composites* 40 (12): 4519–4529. https://doi.org/10.1002/pc.25308.

Bessa, W., D. Trache, M. Derradji, H. Ambar, M. Benziane, and B. Guedouar. 2021. "Effect of Different Chemical Treatments and Loadings of Arundo Donax L. Fibers on the Dynamic Mechanical, Thermal, and Morphological Properties of Bisphenol a Aniline Based Polybenzoxazine Composites." *Polymer Composites* 42 (10): 5199–5208. https://doi.org/10.1002/PC.26215.

Bessa, W., D. Trache, M. Derradji, H. Ambar, A. F. Tarchoun, M. Benziane, B. Guedouar, et al. 2020. "Characterization of Raw and Treated Arundo Donax L. Cellulosic Fibers and Their Effect on the Curing Kinetics of Bisphenol A-Based Benzoxazine." *International Journal of Biological Macromolecules* 164:2931–2943. https://doi.org/10.1016/J.IJBIOMAC.2020.08.179.

Bhattacharjee, S., and D. S. Bajwa. 2018. "Degradation in the Mechanical and Thermo-Mechanical Properties of Natural Fiber Filled Polymer Composites Due to Recycling." *Construction and Building Materials* 172:1–9. https://doi.org/10.1016/j.conbuildmat.2018.03.010.

Brostow, W., H. E. Hagg Lobland, and S. Khoja. 2015. "Brittleness and Toughness of Polymers and Other Materials." *Materials Letters* 159:478–480. https://doi.org/10.1016/j.matlet.2015.07.047.

Chikouche, M. D. L., A. Merrouche, A. Azizi, M. Rokbi, and S. Walter. 2015. "Influence of Alkali Treatment on the Mechanical Properties of New Cane Fibre/Polyester Composites." *Journal of Reinforced Plastics and Composites* 34 (16): 1329–1339. https://doi.org/10.1177/0731684415591093.

Chimeni-Yomeni, D., A. Fazli, C. Dubois, and D. Rodrigue. "Low Density Polyethylene Composites Based on Flax Fibers Modified by a Combination of Coupling Agent." *Polymer Engineering & Science*, https://doi.org/10.1002/pen.26126. n/a(n/a)

Chorobiński, M., Ł. Skowroński, and M. Bieliński. 2019. "Metodyka wyznaczania wybranych charakterystyk barwienia polietylenu z wykorzystaniem systemu CIELab." *Polimery* 64 (10): 690–696. https://doi.org/10.14314/polimery.2019.10.6.

Copani, V., S. L. Cosentino, G. Testa, and D. Scordia. 2013. "Agamic Propagation of Giant Reed (Arundo Donax L.) in Semi-Arid Mediterranean Environment." *Italian Journal of Agronomy* 8 (4): 18–24.

Correa-Aguirre, J. P., F. Luna-Vera, C. Caicedo, B. Vera-Mondragón, and M. A. Hidalgo-Salazar. 2020. "The Effects of Reprocessing and Fiber Treatments on the Properties of Polypropylene-Sugarcane Bagasse Biocomposites." *Polymers* 12 (7): 1440. https://doi.org/10.3390/POLYM12071440.

Cosentino, S. L., C. Patanè, E. Sanzone, G. Testa, and D. Scordia. 2016. "Leaf gas exchange, water status and radiation use efficiency of giant reed (Arundo donax L.) in a changing soil nitrogen fertilization and soil water availability in a semi-arid Mediterranean area." *The European Journal of Agronomy* 72:56–69. https://doi.org/10.1016/j.eja.2015.09.011 .

Cosentino, S. L., D. Scordia, E. Sanzone, G. Testa, and V. Copani. 2014. "Response of Giant Reed (Arundo Donax L.) to Nitrogen Fertilization and Soil Water Availability in Semi-Arid Mediterranean Environment." *The European Journal of Agronomy* 60:22–32. https://doi.org/10.1016/j.eja.2014.07.003.

Dahmardeh Ghalehno, M., M. Madhoushi, T. Tabarsa, and M. Nazerian. 2010. "The Manufacture of Particleboards Using Mixture of Reed (Surface Layer) and Commercial Species (Middle Layer)." *European Journal of Wood and Wood Products* 69 (3): 341–344. https://doi.org/10.1007/S00107-010-0437-7.

Djellali, S., T. Sadoun, N. Haddaoui, and A. Bergeret. 2015. "Viscosity and Viscoelasticity Measurements of Low Density Polyethylene/Poly(lactic Acid) Blends." *Polymer Bulletin* 72 (5): 1177–1195. https://doi.org/10.1007/s00289-015-1331-6.

Dolçà, C. E. Fages, E. Gonga, D. Garcia-Sanoguera, R. Balart, and L. Quiles-Carrillo 2022. "'The Effect of Varying the Amount of Short Hemp Fibers on Mechanical and Thermal Properties of Wood–Plastic Composites from Biobased Polyethylene Processed by Injection Molding'." *Polymers* 14 (1): 138. doi:10.3390/polym14010138.

Dolza, C., E. Fages, E. Gonga, J. Gomez-Caturla, R. Balart, and L. Quiles-Carrillo. 2021. "Development and Characterization of Environmentally Friendly Wood Plastic Composites from Biobased Polyethylene and Short Natural Fibers Processed by Injection Moulding." *Polymers* 13 (11): 1692. https://doi.org/10.3390/polym13111692.

Fendler, A., M. P. Villanueva, E. Gimenez, and J. M. Lagarón. 2007. "Characterization of the Barrier Properties of Composites of HDPE and Purified Cellulose Fibers." *Cellulose* 14 (5): 427–438. https://doi.org/10.1007/s10570-007-9136-x.

Ferrández-García, C. E., J. Andreu-Rodríguez, M. T. Ferrández-García, M. Ferrández-Villena, and T. García-Ortuño. 2012. "Panels Made from Giant Reed Bonded with Non-Modified Starches." *BioResources* 7 (4): 5904–5916. https://doi.org/10.15376/biores.7.4.5904-5916.

Ferrandez-Garcia, M. T., C. E. Ferrandez-Garcia, T. Garcia-Ortuño, A. Ferrandez-Garcia, and M. Ferrandez-Villena. 2019. "Experimental Evaluation of a New Giant Reed (Arundo Donax L.) Composite Using Citric Acid as a Natural Binder." *Agronomy* 9 (12): 882. https://doi.org/10.3390/AGRONOMY9120882.

Ferrandez-García, M. T., A. Ferrandez-Garcia, T. Garcia-Ortuño, C. E. Ferrandez-Garcia, and M. Ferrandez-Villena. 2020. "Assessment of the Physical, Mechanical and Acoustic Properties of Arundo Donax L. Biomass in Low Pressure and Temperature Particleboards." *Polymers* 12 (6): 1361. https://doi.org/10.3390/POLYM12061361.

Ferrández Villena, M., C. E. Ferrández Garcia, T. García Ortuño, A. Ferrández García, and M. T. Ferrández García. 2020. "The Influence of Processing and Particle Size on Binderless Particleboards Made from Arundo Donax L. Rhizome." *Polymers* 12 (3): 696. https://doi.org/10.3390/polym12030696.

Ferrero, B., V. Fombuena, O. Fenollar, T. Boronat, and R. Balart. 2015. "Development of Natural Fiber-Reinforced Plastics (NFRP) Based on Biobased Polyethylene and Waste Fibers from Posidonia Oceanica Seaweed." *Polymer Composites* 36 (8): 1378–1385. https://doi.org/10.1002/pc.23042.

Fiore, V., L. Botta, R. Scaffaro, A. Valenza, and A. Pirrotta. 2014. "PLA Based Biocomposites Reinforced with Arundo Donax Fillers." *Composites Science and Technology* 105:110–117. https://doi.org/10.1016/j.compscitech.2014.10.005.

Fiore, V., T. Scalici, and A. Valenza. 2014. "Characterization of a New Natural Fiber from Arundo Donax L. as Potential Reinforcement of Polymer Composites." *Carbohydrate Polymers* 106 (1): 77–83. https://doi.org/10.1016/j.carbpol.2014.02.016.

Fiore, V., T. Scalici, G. Vitale, and A. Valenza. 2014. "Static and Dynamic Mechanical Properties of Arundo Donax Fillers-Epoxy Composites." *Materials & Design* 57:456–464. https://doi.org/10.1016/j.matdes.2014.01.025.

Gai, J. G., and Y. Cao. 2013. "Structure Memory Effects and Rheological Behaviors of Polyethylenes in Processing Temperature Window." *Journal of Applied Polymer Science* 129 (1): 354–361. https://doi.org/10.1002/app.38754.

García-Ortuño, T., J. Andréu-Rodríguez, M. T. Ferrández-García, M. Ferrández-Villena, and C. E. Ferrández-García. 2011. "Evaluation of the Physical and Mechanical Properties of Particleboard Made from Giant Reed (Arundo Donax L.)." *BioResources* 6 (1): 477–486. https://doi.org/10.15376/biores.6.1.477-486.

George, J., S. S. Bhagawan, and S. Thomas. 1998. "Effects of Environment on the Properties of Low-Density Polyethylene Composites Reinforced with Pineapple-Leaf Fibre." *Composites Science and Technology* 58 (9): 1471–1485. https://doi.org/10.1016/S0266-3538(97)00161-9.

Hejna, A., M. Barczewski, J. Andrzejewski, P. Kosmela, A. Piasecki, M. Szostak, T. Kuang, et al. 2020. "Rotational Molding of Linear Low-Density Polyethylene Composites Filled with Wheat Bran." *Polymers* 12 (5): 1004. https://doi.org/10.3390/POLYM12051004.

Henrique, P., F. Pereira, M. De, F. Rosa, M. Odila, H. Cioffi, D. R. Mulinari, et al. 2015. "Vegetal Fibers in Polymeric Composites: A Review." *Polímeros* 25 (1): 9–22. https://doi.org/10.1590/0104-1428.1722.

Jaramillo, L. Y., M. Vásquez-Rendón, S. Upegui, J. C. Posada, and M. Romero-Sáez. 2021. "Polyethylene-Coffee Husk Eco-Composites for Production of Value-Added Consumer Products." *Sustainable Environment Research* 31 (1): 34. https://doi.org/10.1186/s42834-021-00107-6.

Jensen, E. F., M. D. Casler, K. Farrar, J. M. Finnan, R. Lord, C. Palmborg, Valentine J, and Donnison IS 2018. "Giant Reed: From Production to End Use." In *Perennial Grasses for Bioenergy and Bioproducts*, edited by E. Alexopoulou, 107–150. Amsterdam: Academic Press Inc. Elsevier.

Jyoti, J., B. P. Singh, A. K. Arya, and S. R. Dhakate. 2016. "Dynamic Mechanical Properties of Multiwall Carbon Nanotube Reinforced ABS Composites and Their Correlation with Entanglement Density, Adhesion, Reinforcement and C Factor." *RSC Advances* 6 (5): 3997–4006. https://doi.org/10.1039/C5RA25561A.

Kabir, M. M., H. Wang, K. T. Lau, F. Cardona, and T. Aravinthan. 2012. "Mechanical Properties of Chemically-Treated Hemp Fibre Reinforced Sandwich Composites." *Composites Part B Engineering* 43 (2): 159–169. https://doi.org/10.1016/j.compositesb.2011.06.003.

Karaduman, Y., M. M. A. Sayeed, L. Onal, and A. Rawal. 2014. "Viscoelastic Properties of Surface Modified Jute Fiber/Polypropylene Nonwoven Composites." *Composites Part B Engineering* 67:111–118. https://doi.org/10.1016/j.compositesb.2014.06.019.

Khanna, Y. P., E. A. Turi, T. J. Taylor, V. V. Vickroy, and R. F. Abbott. 1985. "Dynamic Mechanical Relaxations in Polyethylene." *Macromolecules* 18 (6): 1302–1309. https://doi.org/10.1021/ma00148a045.

Koohestani, B., A. K. Darban, P. Mokhtari, E. Yilmaz, and E. Darezereshki. 2019. "Comparison of Different Natural Fiber Treatments: A Literature Review." *International Journal of Environmental Science and Technology* 16 (3): 629–642. https://doi.org/10.1007/s13762-018-1890-9.

Kuan, H. C., J. M. Huang, C. C. M. Ma, and F. Y. Wang. 2003. "Processability, Morphology and Mechanical Properties of Wood Flour Reinforced High Density Polyethylene Composites." *Plastics, Rubber & Composites* 32 (3): 122–126. https://doi.org/10.1179/146580103225001363.

Kubát, J., M. Rigdahl, and M. Welander. 1990. "Characterization of Interfacial Interactions in High Density Polyethylene Filled with Glass Spheres Using Dynamic-Mechanical Analysis." *Journal of Applied Polymer Science* 39 (7): 1527–1539. https://doi.org/10.1002/app.1990.070390711.

Lei, Y., Q. Wu, F. Yao, and Y. Xu. 2007. "Preparation and Properties of Recycled HDPE/Natural Fiber Composites." *Composites Part A: Applied Science and Manufacturing* 38 (7): 1664–1674. https://doi.org/10.1016/j.compositesa.2007.02.001.

Lewandowski, K., K. Piszczek, S. Zajchowski, and J. Mirowski. 2016. "Rheological Properties of Wood Polymer Composites at High Shear Rates." *Polymer Testing* 51:58–62. https://doi.org/10.1016/j.polymertesting.2016.02.004.

Licursi, D., C. Antonetti, J. Bernardini, P. Cinelli, M. B. Coltelli, A. Lazzeri, M. Martinelli, et al. 2015. "Characterization of the Arundo Donax L. Solid Residue from Hydrothermal Conversion: Comparison with Technical Lignins and Application Perspectives." *Industrial Crops and Products* 76:1008–1024. https://doi.org/10.1016/j.indcrop.2015.08.007.

Licursi, D., C. Antonetti, M. Mattonai, L. Pérez-Armada, S. Rivas, E. Ribechini, A. M. Raspolli Galletti, et al. 2018. "Multi-Valorisation of Giant Reed (Arundo Donax L.) to Give Levulinic Acid and Valuable Phenolic Antioxidants." *Industrial Crops and Products* 112:6–17. https://doi.org/10.1016/j.indcrop.2017.11.007.

Martínez-Sanz, M., E. Erboz, C. Fontes, and A. López-Rubio. 2018. "Valorization of Arundo Donax for the Production of High Performance Lignocellulosic Films." *Carbohydrate Polymers* 199:276–285. https://doi.org/10.1016/j.carbpol.2018.07.029.

Mazzanti, V., F. Mollica, and N. El Kissi. 2016. "Rheological and Mechanical Characterization of Polypropylene-Based Wood Plastic Composites." *Polymer Composites* 37 (12): 3460–3473. https://doi.org/10.1002/pc.23546.

Mendes, J. F., J. T. Martins, A. Manrich, B. R. Luchesi, A. P. S. Dantas, R. M. Vanderlei, P. C. Claro, et al. 2021. "Thermo-Physical and Mechanical Characteristics of Composites Based on High-Density Polyethylene (HDPE) E Spent Coffee Grounds (SCG)." *Journal of Polymers and the Environment* 29 (9): 2888–2900. https://doi.org/10.1007/s10924-021-02090-w.

Mohanty, S., and S. K. Nayak. 2010. "Short Bamboo Fiber-Reinforced HDPE Composites: Influence of Fiber Content and Modification on Strength of the Composite." *Journal of Reinforced Plastics and Composites* 29 (14): 2199–2210. https://doi.org/10.1177/0731684409345618.

Molefi, J. A., A. S. Luyt, and I. Krupa. 2010. "Comparison of the Influence of Copper Micro- and Nano-Particles on the Mechanical Properties of Polyethylene/Copper Composites." *Journal of Materials Science* 45 (1): 82–88. https://doi.org/10.1007/s10853-009-3894-9.

Monteiro, S. N., V. Calado, R. J. S. Rodriguez, and F. M. Margem. 2012. "Thermogravimetric Behavior of Natural Fibers Reinforced Polymer Composites—An Overview." *Materials Science and Engineering: A* 557:17–28. https://doi.org/10.1016/j.msea.2012.05.109.

Mysiukiewicz, O., P. Kosmela, M. Barczewski, and H. A. Hejna. 2020. "Mechanical, Thermal and Rheological Properties of Polyethylene-Based Composites Filled with Micrometric Aluminum Powder." *Materials* 13 (5): 1242. https://doi.org/10.3390/ma13051242.

Nabinejad, O. D. Sujan, M. E. Rahman, and I. J. Davies 2015. "'Determination of Filler Content for Natural Filler Polymer Composite by Thermogravimetric Analysis'." *Journal of Thermal Analysis and Calorimetry* 122: 227–233. doi:10.1007/s10973-015-4681-2.

Najafi, S. K., M. Tajvidi, and M. Chaharmahli. 2006. "Long-Term Water Uptake Behavior of Lignocellulosic-High Density Polyethylene Composites." *Journal of Applied Polymer Science* 102 (4): 3907–3911. https://doi.org/10.1002/app.24172.

Ogah, A. O., J. N. Afiukwa, and A. A. Nduji. 2014. "Characterization and Comparison of Rheological Properties of Agro Fiber Filled High-Density Polyethylene Bio-Composites." *OJPChem* 4 (01): 12–19. https://doi.org/10.4236/ojpchem.2014.41002.

Ortega, Z., I. Bolaji, L. Suárez, and E. Cunningham. 2023. "A Review of the Use of Giant Reed (Arundo Donax L.) in the Biorefineries Context". *Reviews in Chemical Engineering*. https://doi.org/10.1515/revce-2022-0069.

Ortega, Z., M. D. Monzón, A. N. Benítez, M. Kearns, M. McCourt, and P. R. Hornsby. 2013. "Banana and Abaca Fiber-Reinforced Plastic Composites Obtained by Rotational Molding Process." *Materials and Manufacturing Processes* 28 (8): 130614085148001. https://doi.org/10.1080/10426914.2013.792431.

Ortega, Z., F. Romero, R. Paz, L. Suárez, A. N. Benítez, and M. D. Marrero. 2021. "Valorization of Invasive Plants from Macaronesia as Filler Materials in the Production of Natural Fiber Composites by Rotational Molding." *Polymers* 13 (13): 2220. https://doi.org/10.3390/POLYM13132220.

Pandey, A. K., R. Kumar, V. S. Kachhavah, and K. K. Kar. 2016. "Mechanical and Thermal Behaviours of Graphite Flake-Reinforced Acrylonitrile–Butadiene–Styrene Composites and Their Correlation with Entanglement Density, Adhesion, Reinforcement and C Factor." *RSC Advances* 6 (56): 50559–50571. https://doi.org/10.1039/C6RA09236E .

Panwar, V., and K. Pal. 2017. "An Optimal Reduction Technique for rGo/ABS Composites Having High-End Dynamic Properties Based on Cole-Cole Plot, Degree of Entanglement and C-Factor." *Composites Part B Engineering* 114:46–57. https://doi.org/10.1016/j.compositesb.2017.01.066.

Patti, A., L. Nele, M. Zarrelli, L. Graziosi, and D. Acierno. 2021. "A Comparative Analysis on the Processing Aspects of Basalt and Glass Fibers Reinforced Composites." *Fibers and Polymers* 22 (5): 1449–1459. https://doi.org/10.1007/s12221-021-0184-x.

Qiu, W., T. Endo, and T. Hirotsu. 2004. "Interfacial Interactions of a Novel Mechanochemical Composite of Cellulose with Maleated Polypropylene." *Journal of Applied Polymer Science* 94 (3): 1326–1335. https://doi.org/10.1002/app.21123.

Salasinska, K., M. Polka, M. Gloc, and J. Ryszkowska. 2016. "Natural Fiber Composites: The Effect of the Kind and Content of Filler on the Dimensional and Fire Stability of Polyolefin-Based Composites." *Polimery* 61 (4): 255–265. https://doi.org/10.14314/polimery.2016.255.

Satapathy, S., and R. V. S. Kothapalli. 2018. "Mechanical, Dynamic Mechanical and Thermal Properties of Banana Fiber/Recycled High Density Polyethylene Biocomposites Filled with Flyash Cenospheres." *Journal of Polymers and the Environment* 26 (1): 200–213. https://doi.org/10.1007/s10924-017-0938-0.

Scalici, T., V. Fiore, and A. Valenza. 2016. "Effect of Plasma Treatment on the Properties of Arundo Donax L. Leaf Fibres and Its Bio-Based Epoxy Composites: A Preliminary Study." *Composites Part B Engineering* 94:167–175. https://doi.org/10.1016/j.compositesb.2016.03.053.

Schellenberg, J. 1997. "Blends of High-Density Polyethylene with Homogeneous Long-Chain Branched Polyethylenes." *Advances in Polymer Technology* 16 (2): 135–145. https://doi.org/10.1002/(SICI)1098-2329(199722)16:2<135:AID-ADV6>3.0.CO;2-V.

Sewda, K., and S. N. Maiti. 2010. "Effect of Teak Wood Flour on Melt Rheological Behaviour of High Density Polyethylene." *Polymer-Plastics Technology and Engineering* 49 (4): 418–425. https://doi.org/10.1080/03602550903413839.

Shatalov, A. A., and H. Pereira. 2013. "High-Grade Sulfur-Free Cellulose Fibers by Pre-Hydrolysis and Ethanol-Alkali Delignification of Giant Reed (Arundo Donax L.) Stems." *Industrial Crops and Products* 43 (1): 623–630. https://doi.org/10.1016/j.indcrop.2012.08.003.

Smitthipong, W., R. Tantatherdtam, and R. Chollakup. 2015. "Effect of Pineapple Leaf Fiber-Reinforced Thermoplastic Starch/Poly(lactic Acid) Green Composite: Mechanical, Viscosity, and Water Resistance Properties." *Journal of Thermoplastic Composite Materials* 28 (5): 717–729. https://doi.org/10.1177/0892705713489701.

Stanciu, M. D., H. Teodorescu Draghicescu, F. Tamas, and O. M. Terciu. 2020. "Mechanical and Rheological Behaviour of Composites Reinforced with Natural Fibres." *Polymers* 12 (6): 1402. https://doi.org/10.3390/polym12061402.

Suárez, L., M. Barczewski, P. Kosmela, M. D. Marrero, and Z. Ortega. 2023. "Giant Reed (Arundo Donax L.) Fiber Extraction and Characterization for Its Use in Polymer Composites." *Journal of Natural Fibers* 20 (1). https://doi.org/10.1080/15440478.2022.2131687.

Suárez, L., J. Castellano, F. Romero, M. D. Marrero, A. N. Benítez, and Z. Ortega. 2021. "Environmental Hazards of Giant Reed (Arundo Donax L.) in the Macaronesia Region and Its Characterisation as a Potential Source for the Production of Natural Fibre Composites." *Polymers 2021* 13 (13): 2101. https://doi.org/10.3390/POLYM13132101.

Suárez, L., Z. Ortega, M. Barczewski, and E. Cunningham. 2023. "Use of Giant Reed (Arundo Donax L.) for Polymer Composites Obtaining: A Mapping Review." *Cellulose* 30 (8): 4793–4812. Published online 2023. https://doi.org/10.1007/s10570-023-05176-x.

Suárez, L., Z. Ortega, F. Romero, R. Paz, and M. D. Marrero. "Influence of Giant Reed Fibers on Mechanical, Thermal, and Disintegration Behavior of Rotomolded PLA and PE Composites." *Journal of Polymers and the Environment* 30 (11): 4848–4862. https://doi.org/10.1007/s10924-022-02542-x.

Tarchoun, A. F., D. Trache, T. M. Klapötke, M. Derradji, and W. Bessa. 2019. "Ecofriendly Isolation and Characterization of Microcrystalline Cellulose from Giant Reed Using Various Acidic Media." *Cellulose* 26 (13–14): 7635–7651. https://doi.org/10.1007/s10570-019-02672-x.

Wang, K., F. Addiego, A. Laachachi, B. Kaouache, N. Bahlouli, V. Toniazzo, and D. Ruch. 2014. "Dynamic Behavior and Flame Retardancy of HDPE/Hemp Short Fiber Composites: Effect of Coupling Agent and Fiber Loading." *Composite Structures* 113:74–82. https://doi.org/10.1016/j.compstruct.2014.03.009.

Wang, W., M. Sain, and P. A. Cooper. 2006. "Study of Moisture Absorption in Natural Fiber Plastic Composites." *Composites Science and Technology* 66 (3): 379–386. https://doi.org/10.1016/j.compscitech.2005.07.027.

Zhang, F., T. Endo, W. Qiu, L. Yang, and T. Hirotsu. 2002. "Preparation and Mechanical Properties of Composite of Fibrous Cellulose and Maleated Polyethylene." *Journal of Applied Polymer Science* 84 (11): 1971–1980. https://doi.org/10.1002/app.10428.